

Synthesis and Evaluation of Indenopyrazoles as Cyclin-Dependent Kinase Inhibitors. 3. Structure Activity Relationships at C3^{1,2}

Eddy W. Yue,* C. Anne Higley, Susan V. DiMeo, David J. Carini, David A. Nugiel, Carrie Benware, Pamela A. Benfield, Catherine R. Burton, Sarah Cox, Robert H. Grafstrom, Diane M. Sharp, Lisa M. Sisk, John F. Boylan, Jodi K. Muckelbauer, Angela M. Smallwood, Haiying Chen, Chong-Hwan Chang, Steven P. Seitz, and George L. Trainor

Bristol-Myers Squibb Company, Experimental Station, P.O. Box 80500, Wilmington, Delaware 19880-0500

Received April 22, 2002

The identification of indeno[1,2-c]pyrazol-4-ones as inhibitors of cyclin-dependent kinases (CDKs) has led to the discovery of a series of novel and potent compounds. Herein, we report the effects of substitutions at C3 of the indeno[1,2-c]pyrazol-4-one core with alkyls, heterocycles, and substituted phenyls. Substitutions at the para position of the phenyl ring at C3 were generally well-tolerated; however, larger groups were generally inactive. For alkyls directly attached to C3, longer chain substituents were not tolerated; however, shorter alkyl groups and cyclic alkyls were acceptable. In general, the heterocycles at C3 gave the most potent analogues. One such heterocycle, **24j**, was examined in detail and was determined to have a biological profile consistent with CDK inhibition. An X-ray crystal structure of one of the alkyl compounds, **13q**, complexed with CDK2 was determined and showed the inhibitor residing in the adenosine 5'-triphosphate pocket of the enzyme.

Introduction

Cyclin-dependent kinase (CDK) inhibitors have garnered attention recently for their potential as anticancer therapeutics.³ CDKs are cellular kinases, which play a crucial role in the regulation of progression through the different phases of the cell cycle. As their name implies, each of these kinases requires the association with a cyclin in order for it to become active. Several CDK/cyclin pairs have been identified, which have key roles in the cell cycle machinery including CDK4/D1, CDK2/E, CDK2/A, and CDK1/B.^{4–6} Because cell cycle dysregulation is a characteristic of transformed cells, it has been theorized that inhibition of certain CDK/cyclin complexes would be of value in the treatment of proliferative diseases.

The search for small molecule inhibitors of CDKs has already led to the discovery of several classes of compounds including butyrolactone I,⁷ the flavonoids represented by flavopiridol,^{8,9} and purines such as olomoucine,^{10,11} roscovitine,^{12,13} and purvalanol¹⁴ (Figure 1). Butyrolactone I is an inhibitor of CDK1 and CDK2 with selectivity over other non-CDK kinases. Flavopiridol has activity for several CDKs including CDK1, CDK2, and CDK4 and has shown efficacy in animal tumor models. Flavopiridol is currently undergoing clinical trials as a cell cycle inhibitor for the treatment of cancer. Olomoucine has modest activity for CDK1 and CDK2 but is inactive against CDK4. Roscovitine, purvalanol A, and purvalanol B are more potent purine analogues with selectivity for CDK2 and CDK5 vs CDK4 and several other kinases. The last four examples suggest that some selectivity within the CDK family can be achieved.

More recent reports of CDK inhibitors have included several novel classes of compounds including the indoli-

nones,¹⁵ pyridopyrimidinones,¹⁶ and aminothiazoles¹⁷ (Figure 1). GW8510 is a representative of the indolinones with good potency in CDK2 and with selectivity against CDK1 and CDK4. The pyridopyrimidinone PD172803 and the aminothiazole AG12286 both showed good potency against CDK4/D and CDK2/A.

We have previously disclosed our investigations into the novel indenopyrazole class of CDK inhibitors, which centered around the optimization of the C5 aniline substituent^{18,19} (Figure 2). Earlier analogues employed a 4-methoxyphenyl group at C3, and we were particularly interested in the effects of alternately substituted phenyl groups as well as heterocycles and alkyls in this position. In this paper, we present our findings on the impact of a variety of substitutions at C3.

Chemistry

The synthesis of indenopyrazoles substituted at C3 involved two different routes. For C3 para-substituted phenyls, the chemistry previously described¹⁹ was utilized. Condensation of diester **2** with an acetophenone appropriately substituted at the para position gave the triketones **4** in good yield (Scheme 1). Cyclization of the triketones using hydrazine provided the desired indenopyrazoles with a C5 acetamide (**5**). Glycinamides at C5 were prepared by removal of the acetamide (**5** → **6**), formation of the α -chloroacetamide (**6** → **7**), and condensation with the appropriate amine (**7** → **8**).

The conditions developed for the synthesis of C3 aryl analogues were incompatible with the C3 alkyl substrates. Attempts to synthesize the triketone using **2** and the 1,1-dimethylhydrazone of 2-butanone also failed. The synthesis of triketones with C3 alkyl groups, however, was accomplished using a procedure developed by Rotberg and Oshkaya.²⁰ Condensation of 3-nitrophthalic anhydride with symmetrical 1,3-diones in acetic anhydride and triethylamine gave the 4-nitro-1,3-

* To whom correspondence should be addressed. Tel: (302)467-6054. Fax: (302)467-6951. E-mail address: eddy.yue@bms.com.

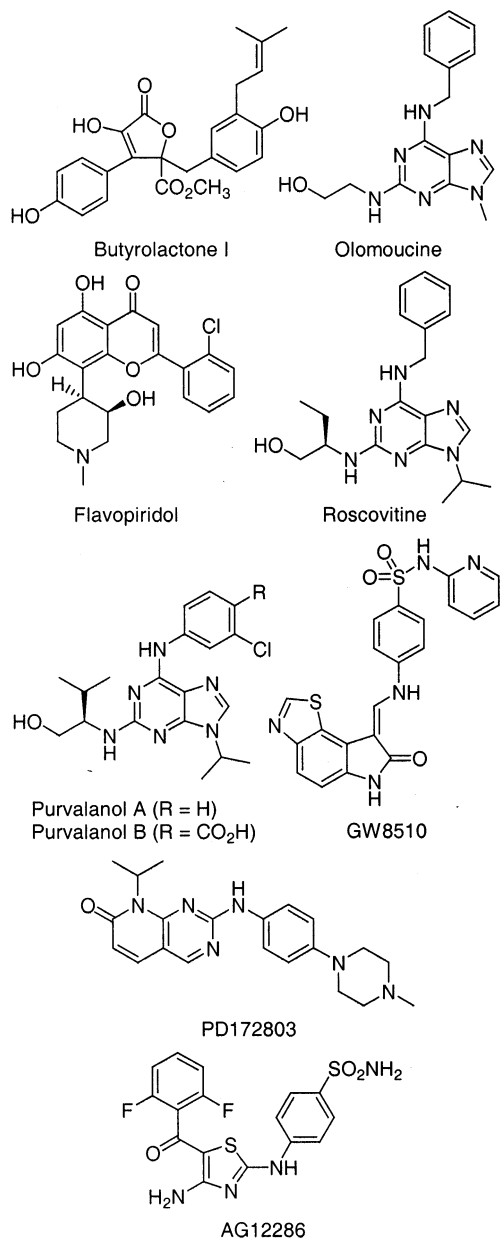


Figure 1. Structures of CDK inhibitors.

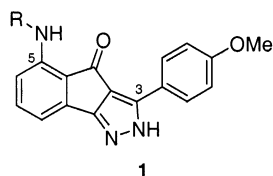


Figure 2. Structures of indenopyrazole **1**.

indanediones **10** in good yields (Scheme 2). Reduction of the nitro group with zinc and calcium chloride provided the desired aniline **11** with no sign of overreduced materials. Acetylation of the aniline produced the triketone precursor **12**, which was cyclized to give the desired pyrazole **13** with alkyl substituents at C3.

The use of symmetrical 1,3-diones for the phthalic anhydride condensation was efficient for smaller alkyl groups, but as the substitutions increased in size and complexity, the yields for the reaction decreased. To circumvent this problem, the use of unsymmetrical 1,3-diones was explored. For unsymmetrical ketones of type

20 (R = alkyl group to be transferred and R' = methyl or trifluoromethyl), it was discovered that selective elimination of the acetyl or trifluoroacetyl group could be achieved (Scheme 3). This simplified the synthesis of analogues to the preparation of unsymmetrical 1,3-diketones **20**, which were easily prepared from the corresponding ketones (**19**).

In an attempt to generate a late-stage intermediate to facilitate the derivatization of the C5 aniline, the formation of the indenopyrazole core from the nitrotriketone (**10**) intermediate was investigated. Cyclization of nitrotriketone **10a** (R = Me) with hydrazine in refluxing ethanol did not produce any desired pyrazole but afforded exclusively the hydrazone **14** (Scheme 2). This phenomenon seemed to be confined to the alkyl analogues since cyclization of the substituted phenyls and heterocycles all proceeded in ethanol. To induce cyclization, elevated temperatures were tried. When the triketone **10a** as well as the hydrazone **14** were subjected to the same conditions using higher boiling *n*-butanol, the cyclized pyrazole was formed but as the undesired 8-nitro regioisomer **15**. This was in contrast to the previously reported cyclizations of acetamide-bearing substrates, which gave the desired 5-position substitution.¹⁹ The regiochemistry of this 8-nitro compound was confirmed by converting the nitro group to the 8-acetamide (**17**) via the aniline (**16**) and comparing this compound with that of the desired 5-acetamide compound **13a**.

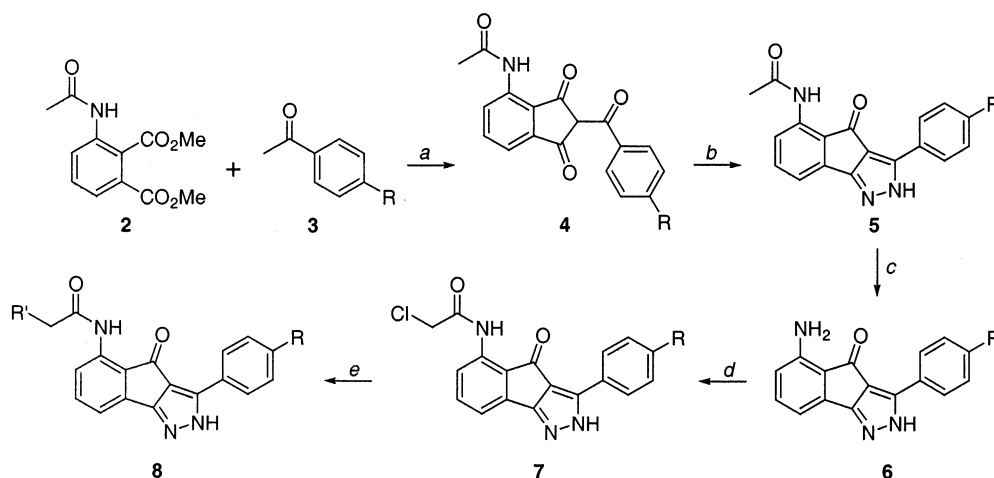
Although disappointing, the regiochemistry of the cyclization was not surprising since the nitro group would be expected to enhance the electrophilic nature of the carbonyl ortho to the nitro group (**14** → **15**). In the case of the acetamide, the carbonyl ortho to the acetamide functionality would have reduced reactivity due to its conjugation with the aniline as a vinylogous amide (Figure 3) and therefore gives the desired cyclized product (**21** → **13a**).

Glycinamides at the 5-position in the C3 alkyl series were prepared using the chemistry described for the para-substituted phenyl analogues.¹⁹ Formation of the chloroacetamide **18** proceeded in good yield (Scheme 2). Displacement of the chlorine with 4-aminomethylpiperidine or isonipecotamide gave the desired triketones, which were cyclized to the pyrazole analogues.

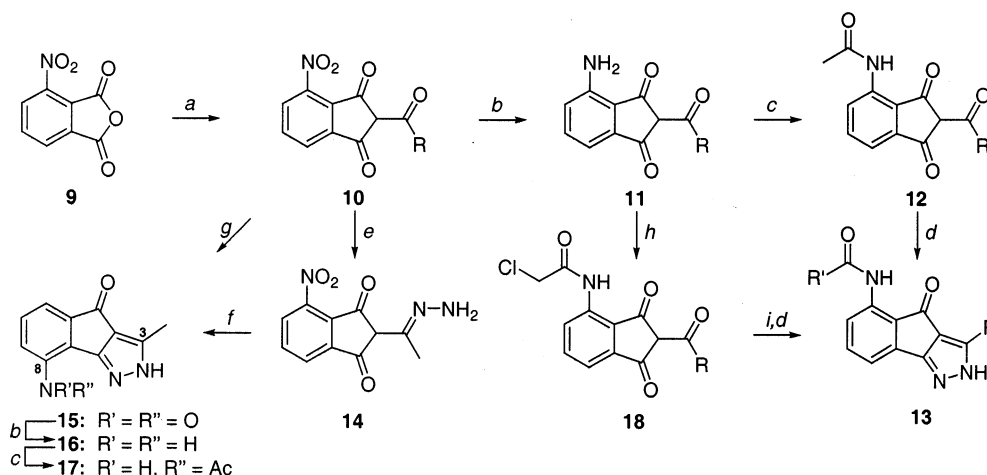
Ureas at the 5-position for both the C3 alkyl and the heterocycle series were prepared according to the previously disclosed indenopyrazole chemistry.¹⁹ Treatment of the aniline **11** with phenylchloroformate gave the carbamate **22** in good yield (Scheme 4). Addition of ammonium hydroxide to the carbamate generated the desired urea triketones **23**, which were cyclized under standard conditions to the pyrazole **24**.

Results and Discussions

C3 *para*-Phenyl Substituents. The optimization at C3 began with an examination of the para position of the C3 phenyl group. A number of substituents were tolerated at the para position (Table 1). With the alkyl-substituted analogues, the activity in both CDK4/D1 and CDK2/E steadily decreased from methyl and ethyl to longer chain alkyls such as propyl and butyl. The same pattern was also observed with the oxygenated variants; methoxy was tolerated, but ethoxy, phenoxy,

Scheme 1^a

^a Reagents: (a) NaH, DMF, 90 °C. (b) H₂NNH₂, EtOH, reflux. (c) Concentrated HCl, MeOH, reflux. (d) ClCH₂COCl, 2.5 M Na₂CO₃(aq), dioxane, 50 °C. (e) 2° amine, EtOH, reflux.

Scheme 2^a

^a Reagents: (a) RC(=O)CH₂C(=O)R' (**20**), Ac₂O, Et₃N, 25 °C. (b) Zn, CaCl₂, EtOH, H₂O, reflux. (c) AcCl, Na₂CO₃, acetone, 50 °C. (d) H₂NNH₂, BuOH, reflux. (e) H₂NNH₂, EtOH, reflux. (f) BuOH, reflux. (g) H₂NNH₂, BuOH, reflux. (h) ClCH₂C(=O)Cl, Na₂CO₃, acetone, 50 °C. (i) 4-Aminomethylpiperidine or isonipecotamide, EtOH, 100 °C sealed tube.

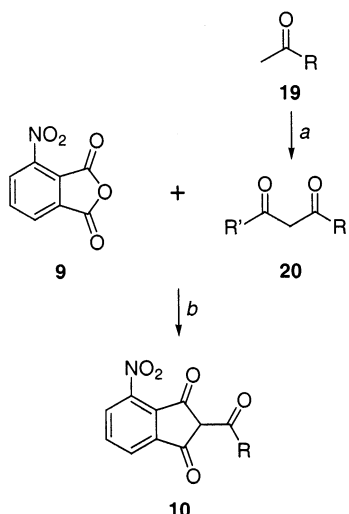
and benzyloxy all gave decreased activity in both CDK4/D1 and CDK2/E. In both of these series of compounds, the smaller para substituents, methyl (**5b**) and methoxy (**5g**), were clearly favored.

In the aniline series, the dimethylamino analogue **5j** had potency similar to the methoxy group and again there was a slight loss in activity with larger groups at that position. The piperidino (**5k**) and morpholino (**5l**) analogues were both less active in CDK4/D1. Interestingly, although **5k** was also less active in CDK2/E as compared with **5j**, **5l** was essentially unchanged and suggested that cyclic groups could be tolerated at that position. The thio derivative **5m** followed the trend of the other small groups with activity similar to that of the methyl compound **5b**.

Although the *p*-dimethylaminophenyl (**5j**) and *p*-morpholinophenyl (**5l**) analogues were similar in activity to *p*-methoxyphenyl (**5g**), it was reasoned that these compounds might provide improved solubility; therefore, these analogues were further pursued. A series of glycinamides were synthesized and for those containing *p*-dimethylaminophenyl at C3 (**8a–d**), there was a marked increase in activity in CDK2/E for all of the

analogues as compared with the parent acetamide **5j** (Table 2). In CDK4/D1, however, the results were dependent on the groups used. The morpholino (**8a**), hydroxy piperidine (**8b**), and methyl piperazine (**8d**) glycinamides were slightly more active than the acetamide **5j**, but the aminomethylpiperidine (**8c**) gave a significant improvement in CDK4/D1 activity. The *p*-morpholinophenyl glycinamides were either the same (**8e**) or slightly worse (**8f–h**) against CDK4/D1 and CDK2/E as compared with the *p*-dimethylaminophenyl derivatives (Table 2). The aminomethylpiperidine analogue **8g**, however, again proved to be a good inhibitor of CDK4/D1 with similar activity in CDK2/E. These results were consistent with previous work, which showed that a *p*-methoxyphenyl at C3 combined with the aminomethylpiperidine glycinamide at C5 gave a very potent CDK4/D1 inhibitor with balanced CDK2/E activity (CDK4/D1 IC₅₀ = 13 nM, CDK2/E IC₅₀ = 14 nM).¹⁹

C3 Alkyl Substituents. Intrigued by the results of the para-substituted phenyl compounds, the phenyl group was removed and analogues that had an alkyl group directly attached to the C3 position were next

Scheme 3^a

^a Reagents: (a) F_3CCO_2Et , Na, EtOH, 25 °C. (b) Ac_2O , Et_3N , 25 °C.

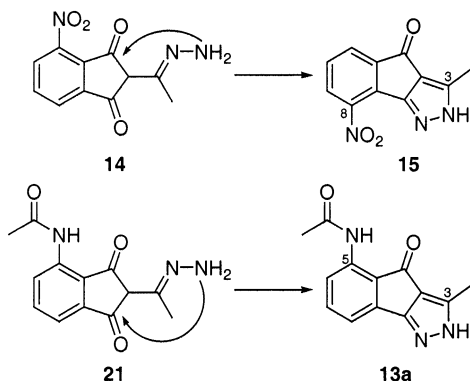
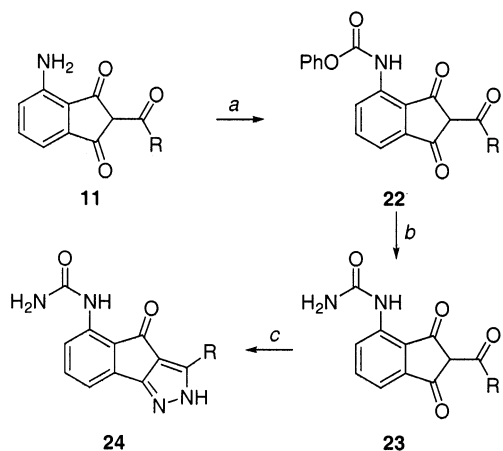


Figure 3. Proposed pathways for the cyclization of the 5-nitro and 5-acetamido triketones to the indenopyrazole core.

Scheme 4^a

^a Reagents: (a) $PhOC(=O)Cl$, Na_2CO_3 , acetone, 50 °C. (b) NH_4OH , DMSO, 90 °C. (c) H_2NNH_2 , EtOH, reflux.

examined. A series of C3 alkyl substituents with C5-acetamides were all inactive against CDK4/D1 (Table 3). CDK2/E was significantly more tolerant of aliphatic substituents. A large increase in activity was observed in going from methyl to ethyl with further improvement when branching was added to give the isopropyl analogue. Longer chain compounds such as the *n*-butyl and *i*-butyl lost inhibitory activity. The larger but con-

Table 1. C3 *para*-Phenyl, C5 Acetamide SAR

compd	R	IC ₅₀ (nM)	
		CDK4/D1 ^a	CDK2/E ^a
5a	H	840	240
5b	Me	490	160
5c	Et	640	280
5d	<i>n</i> -Pr	1900	490
5e	<i>n</i> -Bu	>2800	>560
5f	OH	2300	530
5g	OMe	450	270
5h	OEt	>580	>400
5i	OPh	>2500	>2500
5j	NMe ₂	310	320
5k	piperidino	680	900
5l	morpholino	860	370
5m	SMe	340	120

^a Values correspond to $n = 2$.

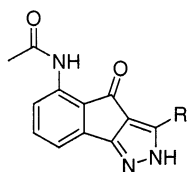
Table 2. C3 *para*-Phenyl, C5 Glycinamide SAR

compd	R'	R	IC ₅₀ (nM)	
			CDK4/D1 ^a	CDK2/E ^a
8a		NMe ₂	110	36
8b		NMe ₂	50	33
8c		NMe ₂	7	15
8d		NMe ₂	55	29
8e		mor-pholino	120	37
8f		mor-pholino	110	85
8g		mor-pholino	18	26
8h		mor-pholino	190	42

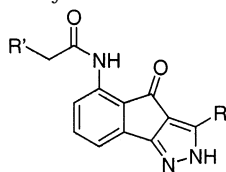
^a Values correspond to $n = 2$.

strained *c*-hexyl was also active, which led to the conclusion that for straight chain analogues, a two carbon length was optimal; however, larger groups could also be accommodated if they have restricted conformations. These results were largely in line with the *para*-substituted phenyl series, which also showed a preference for smaller or cyclic substituents. It was clear, though, that the phenyl spacer did provide an increase in activity especially against CDK4/D1.

Next to be profiled were aliphatic C3 substituents with the more potent C5 glycinamides. The nipecotamide glycinamides provided a large increase in potency for the *i*-propyl (**13k**), *c*-propyl (**13l**), and *c*-hexyl (**13m**) compounds in CDK2/E (Table 4). Similar improvements were seen with the 4-aminomethylpiperidine glycinamides. In addition, the solubility of these compounds at pH 7.4 (*i*-propyl (**13o**) = 1.23 mg/mL, *c*-propyl (**13p**)

Table 3. C3 Alkyl, C5 Acetamide SAR

compd	R	IC ₅₀ (nM)	
		CDK4/D1 ^a	CDK2/E ^a
13a	Me	>4200	11000
13b	Et	>3900	1500
13c	<i>n</i> -Pr	>3700	>3700
13d	<i>i</i> -Pr	>3700	840
13e	<i>c</i> -Pr	>3700	480
13f	<i>i</i> -Bu	>3500	>3500
13g	<i>n</i> -Bu	>3500	>3500
13h	<i>t</i> -Bu	>3500	980
13i	<i>c</i> -Hx	>3200	1100

^a Values correspond to *n* = 2.**Table 4.** C3 Alkyl, C5 Glycinamide SAR

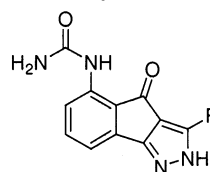
compd	R'	R	IC ₅₀ (nM)	
			CDK4/D1 ^a	CDK2/E ^a
13j	H ₂ NOC-(piperazine)	Et	>2600	>130
13k	H ₂ NOC-(piperazine)	<i>i</i> -Pr	>1300	21
13l	H ₂ NOC-(piperazine)	<i>c</i> -Pr	>99	26
13m	H ₂ NOC-(piperazine)	<i>c</i> -Hx	>570	36
13n	H ₂ N-(piperazine)	Et	1300	240
13o	H ₂ N-(piperazine)	<i>i</i> -Pr	340	48
13p	H ₂ N-(piperazine)	<i>c</i> -Pr	430	55
13q	H ₂ N-(piperazine)	<i>c</i> -Hx	360	96

^a Values correspond to *n* = 2.

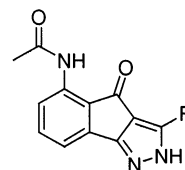
> 0.87 mg/mL, and *c*-hexyl (**13q**) > 0.6 mg/mL) was quite good as compared with those of the C3 phenyl analogues. Comparison of **13o** with **8g** (0.01 mg/mL) and **8c** (0.001 mg/mL) shows an increase in solubility of more than 100-fold.

From previous work, it was suggested that further improvements in activity could be made by incorporating ureas at C5.¹⁹ Even though the primary ureas (**24a–d**) showed a marked improvement in activity as compared with the 5-acetamides, they were in general less potent than the substituted acetamides (Table 5). In addition, these ureas (**24a–d**) were all quite insoluble at pH 7.4 (<0.01 mg/mL).

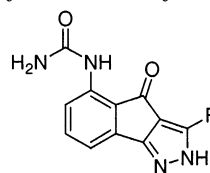
C3 Heterocycle Substituents. The next series of compounds to be examined were the C3 heterocycles (Table 6). With an acetamide at the 5-position, all of the examples were less active in CDK4/D1 as compared with the unsubstituted phenyl derivative **5a**. In CDK2/E, the 3-pyridyl analogue (**13r**) was less potent than the phenyl analogue (**5a**) but the 4-pyridyl compound (**13s**)

Table 5. C3 Alkyl, C5 Primary Urea SAR

compd	R	IC ₅₀ (nM)	
		CDK4/D1 ^a	CDK2/E ^a
24a	Et	>2000	290
24b	<i>i</i> -Pr	>1900	84
24c	<i>c</i> -Pr	1400	140
24d	<i>c</i> -Hx	>810	140

^a Values correspond to *n* = 2.**Table 6.** C3 Heterocycle, C5 Acetamide SAR

compd	R	IC ₅₀ (nM)	
		CDK4/D1 ^a	CDK2/E ^a
13r	3-pyridyl	>1600	770
13s	4-pyridyl	1300	76
13t	2-thienyl	4500	180
13u	2-thienyl, 3-Me	>3100	260
13v	3-thienyl, 2,5-diCl	>2600	>2600
13w	2-furanyl	>3500	>1700

^a Values correspond to *n* = 2.**Table 7.** C3 Heterocycle, C5 Primary Urea SAR

compd	R	IC ₅₀ (nM)	
		CDK4/D1 ^a	CDK2/E ^a
24e	2-thienyl	150	11
24f	2-thienyl, 3-Me	350	17
24g	2-thienyl, 5-Me	53	13
24h	2-thienyl, 5-CO ₂ Et	300	130
24i	3-thienyl	67	9
24j	3-thienyl, 5-Cl	57	13
24k	3-thienyl, 2,5-diMe	>1500	61
24l	2-furanyl	840	86
24m	3-pyrrolyl, 1-Me	130	26

^a Values correspond to *n* = 2.

was more active suggesting the presence of a specific binding interaction, which was optimal at the para position. The 2-thienyl compound proved a little better than phenyl for CDK2/E. The 3-methyl-2-thienyl analogue was about equipotent in CDK2/E as compared with phenyl, but the 2,5-dichloro-3-thienyl and 2-furanyl were both inactive.

Encouraged by these results, primary ureas at C5 were examined. The 2-thienyl compound **24e** was a potent inhibitor in CDK2/E with modest activity in CDK4/D1 (Table 7). There was a slight loss in activity with 2-furanyl (**24l**) in CDK2/E and CDK4/D1, and the 1-methyl-3-pyrrolyl analogue (**24m**) was about the same

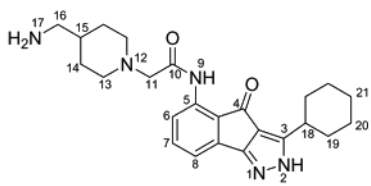
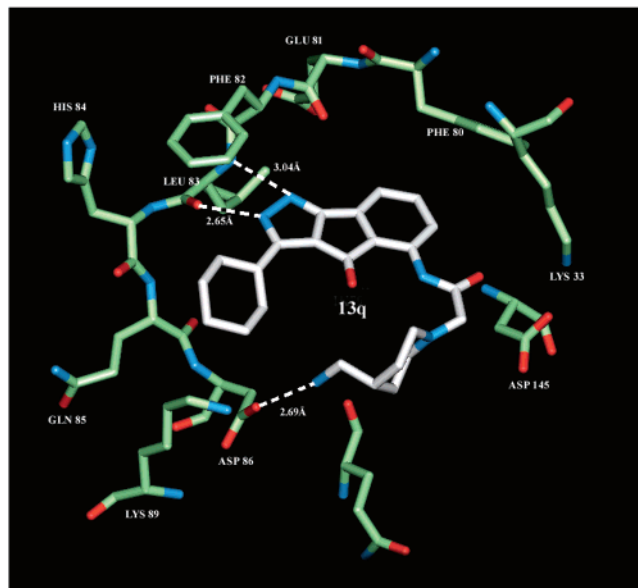


Figure 4. Structure of **13q** in the CDK2 ATP binding pocket. Protein carbons are colored light green, and inhibitor carbons are colored white.

as the 2-thienyl compound. With the 2-thienyl as the starting point, substitutions around the thiophene ring were examined. When a methyl substituent was added to the 3-position of the 2-thienyl group, the potency dropped with a slight loss in both CDK2/E and CDK4/D1 (**24f**). A 5-methyl group gave comparable activity for CDK2/E, but it also showed a slight improvement in activity for CDK4/D1 (**24g**). There seemed to be some requirements for the groups that can be accommodated in the 5-position of the thiophene. For example, the 5-ethyl ester (**24h**) decreased the activity in both CDK2/E and CDK4/D1 as compared with the 5-methyl group (**24g**).

In going from a 2-thienyl to a 3-thienyl system, an improvement in CDK4/D1 was again noticed. Compound **24i** gave a slight increase in activity for CDK4/D1 as compared with the 2-thienyl (**24e**) whereas the CDK2/E remained the same. The 5-chloro-3-thienyl compound (**24j**) was also prepared, and it was comparable to the 3-thienyl. Interestingly, the 2,5-dimethyl-3-thienyl derivative (**24k**) lost most of the CDK4/D1 activity while maintaining CDK2/E potency.

X-ray Crystal Structure of 13q. To determine the binding mode of these inhibitors, an X-ray crystal structure of **13q** complexed to CDK2 was obtained (1.85 Å resolution). Compound **13q** binds into the adenosine 5'-triphosphate (ATP) binding pocket of CDK2 and shares the same bidentate hydrogen bond with Leu83 as seen in other CDK2 inhibitors.^{12,14,16,21–26} Both nitrogens of the indenopyrazole core of **13q** are involved in the hydrogen bonds with Leu83. The distance of N1 with the backbone nitrogen of Leu83 is 3.04 Å and that of N2 with the backbone oxygen of Leu83 is 2.65 Å. The

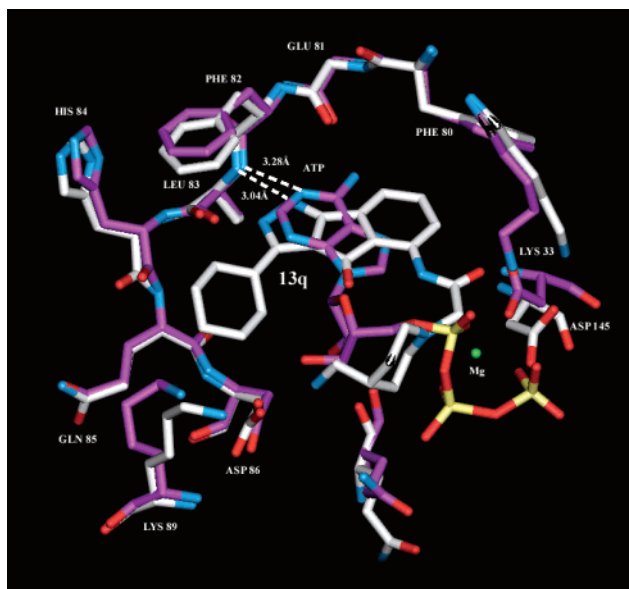


Figure 5. Superposition of **13q** and ATP²⁷ complexed to CDK2. The CDK2/**13q** carbons are colored white, and the CDK2/ATP carbons are colored purple. The magnesium atom from the CDK2/ATP structure²⁷ is colored green.

structure of **13q** folds back onto itself in a U shape conformation, which brings the C3 cyclohexyl and the C5 glycinamide groups in close proximity. This conformation results in the cyclohexyl and glycinamide groups pointing toward the exterior of the protein and hence are partially exposed to solvent. It also results in the formation of a hydrogen bond between N17 of the glycinamide group and the side chain oxygen of Asp 86 (Figure 4). The conformation of the C5 amide is coplanar with the carbonyl at C4, which allows the hydrogen of N9 to form an intramolecular hydrogen bond to the carbonyl (2.89 Å). This is consistent with the proton shift of the N9 hydrogen in the NMR spectra of **13q** (δ 11.19) as well as in other analogues. The indenopyrazole core occupies the same region as the adenine ring of ATP, and the hydrogen bond between Leu83 and N1 of **13q** mimics the hydrogen bond between the same backbone nitrogen and the adenine ring of ATP (Figure 5).^{27,28} Other residues within 3.5 Å of **13q** are Ile10, Lys 33, Lys 89, Gln 131, and Asp145.

Although this X-ray structure does not include bound cyclin, the differences in the ATP binding site of CDK2 are minimal and, therefore, provide useful information for the understanding of how these inhibitors bind in the active site. The crystal structure of **13q** indicates that there is space to accommodate groups at C3 of the indenopyrazole core. This is consistent with the CDK2/E enzyme binding data, which showed a variety of different substituents gave good activity; however, straight chain alkyl groups directly attached to the indenopyrazole core at C3 were not good binders. Because the C3 substituents point to the exterior of the protein, bulkier groups that fill the pocket and maximize van der Waals interactions might be less exposed to solvent as compared with linear alkyl groups. This was also evident in the para-substituted phenyl series in which the activity decreased from methyl (**5b**) to longer chain alkyls (**5c–e**). The *p*-phenoxy phenyl analogue (**5i**) had poor activity, which suggests large hydrophobic groups that extend too far out into the solvent-exposed areas

Table 8. Cellular Activity of Selected Compounds

compd	IC ₅₀ (nM)		
	HCT116 ^a	CDK4/D1 ^a	CDK2/E ^a
8c	74	7	15
8g	110	18	26
13k	290	> 1300	21
13l	120	> 99	26
24e	41	150	11
24f	140	350	17
24g	29	53	13
24i	360	67	9
24j	130	57	13
24m	64	130	26

^a Values correspond to *n* = 2.**Table 9.** Enzymatic and Cellular Activity of **24j**

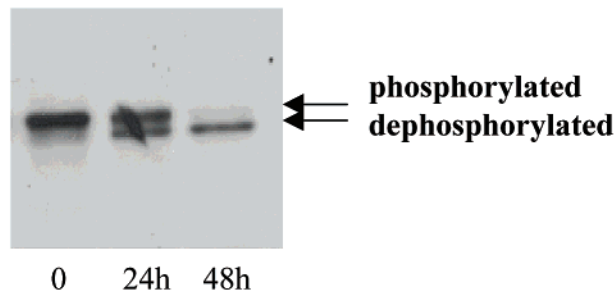
	IC ₅₀ (nM) ^a
CDK1/B	44
c-abl	> 60000
PKA	> 58000
PKC	> 58000
AG1523 (arrested)	EC ₅₀ > 29000
B16-F1	200
HT29	> 2900
HT1080	490
MiaPaCa2	260
NCI-H460	240
PC3	690

^a Values correspond to *n* = 2.

lead to poor binding. The similarly sized *p*-piperidino (**5k**) and *p*-morpholino (**5l**) derivatives are more hydrophilic and, therefore, interact more favorably as evidenced by their increased binding (Table 1).

The enzyme data also showed that substituted glycinamides at C5 usually gave better potency than the smaller acetamides. The close proximity of the C5 glycinamide group in **13q** with the C3 cyclohexyl group may add to the stability of the complex by increasing the number of van der Waals interactions while decreasing exposure to solvent. In addition, the greater steric bulk of the glycinamides may contribute to increased binding by occupying more of the pocket. As can be seen from the CDK2/E enzyme binding data, there was not much difference in activity between the glycinamides as they showed similar potencies (Table 2). Primary ureas at C5 also had good activity in the CDK2/E enzyme assay even though their size resembles the acetamides more than the glycinamides.

Cellular Activity. The most active compounds in CDK4/D1 and CDK2/E were assayed in an HCT116 colon carcinoma-derived cell line. The translation of the enzymatic activity into cellular potency was quite good (Table 8). In general, the heterocycles were more potent than the substituted phenyls and alkyls and several compounds showed interesting activity against HCT116. Compound **24j** represented one of the more potent inhibitors, and it appeared to have differential activity on tumor cells as compared to arrested normal human fibroblasts. As shown in Table 9, the difference in activity of **24j** against HCT116 vs the normal human fibroblast AG1523 is greater than 230-fold. This large gap in activity for proliferating tumor cells vs arrested normal cells was deemed important as it might lead to a potentially useful therapeutic window in vivo. For this reason, the cellular properties of **24j** were examined in more detail.

**Figure 6.** Treatment of asynchronous AG1523 with 1.45 μ M **24j** results in Rb dephosphorylation.

First, **24j** was tested for its inhibitory activity against a broader panel of kinase targets (Table 9). Compound **24j** showed good selectivity (> 1000-fold) for CDK targets as compared with non-CDK targets. Good inhibitory activity (IC₅₀ < 100 nM) was observed against each of the three major cell cycle CDK targets tested with maximum potency being recorded against CDK2/E (IC₅₀ = 13 nM). The compound was approximately 4-fold less potent on CDK4/D1 (IC₅₀ = 57 nM) and CDK1/B (IC₅₀ = 44 nM).

Second, **24j** was tested for inhibitory potency against a broader panel of human and murine tumor cell lines. The compound showed good inhibitory activity against each of the additional six cell lines tested with IC₅₀ values in the 200–690 nM range. One exception was the HT29 human colon carcinoma cell line, which appeared unresponsive to **24j** treatment (IC₅₀ > 2900 nM).

Compound **24j** was further tested to determine if it had cell cycle effects consistent with its profile of CDK inhibition. These experiments were performed in normal human fibroblasts (AG1523) to avoid confounding effects of loss of checkpoint control in tumor-derived cell lines. Treatment of subconfluent, asynchronously proliferating AG1523 with 1.45 μ M **24j** resulted in loss of phosphorylated retinoblastoma (Rb), a CDK substrate, as indicated by a slight increase in mobility on polyacrylamide gel electrophoresis (PAGE). Loss of phosphorylated substrate was apparent within 24 h of treatment and complete by 48 h (Figure 6). Cell cycle progression experiments were designed to examine synchronized cell populations through one transit of the cell cycle (AG1523 doubling time is approximately 60 h, data not shown). The impact of **24j** on G1 progression in these cells was tested by treatment of cells released from a G1 block. The cells were arrested in G1 by growing to confluence. Cells were stimulated to reenter the cell cycle by subculture at lower density and followed by FACS analysis for a 48 h period. At no time during the 48 h observation period were cells arrested through contact inhibition. Within 24 h of serum treatment, significant progression of cells into G2/M had occurred in vehicle-treated control cells as judged by FACS analysis (Figure 7, panel 4). This cell cycle progression is almost completely inhibited in cells treated with 348 nM **24j** and is totally blocked in cells treated with 10-fold higher levels of compound. This is the expected response of cells to a compound capable of inhibiting CDK4/D1 and CDK2/E. The concentration of **24j** at which cell cycle progression is inhibited (approximately 350 nM) is

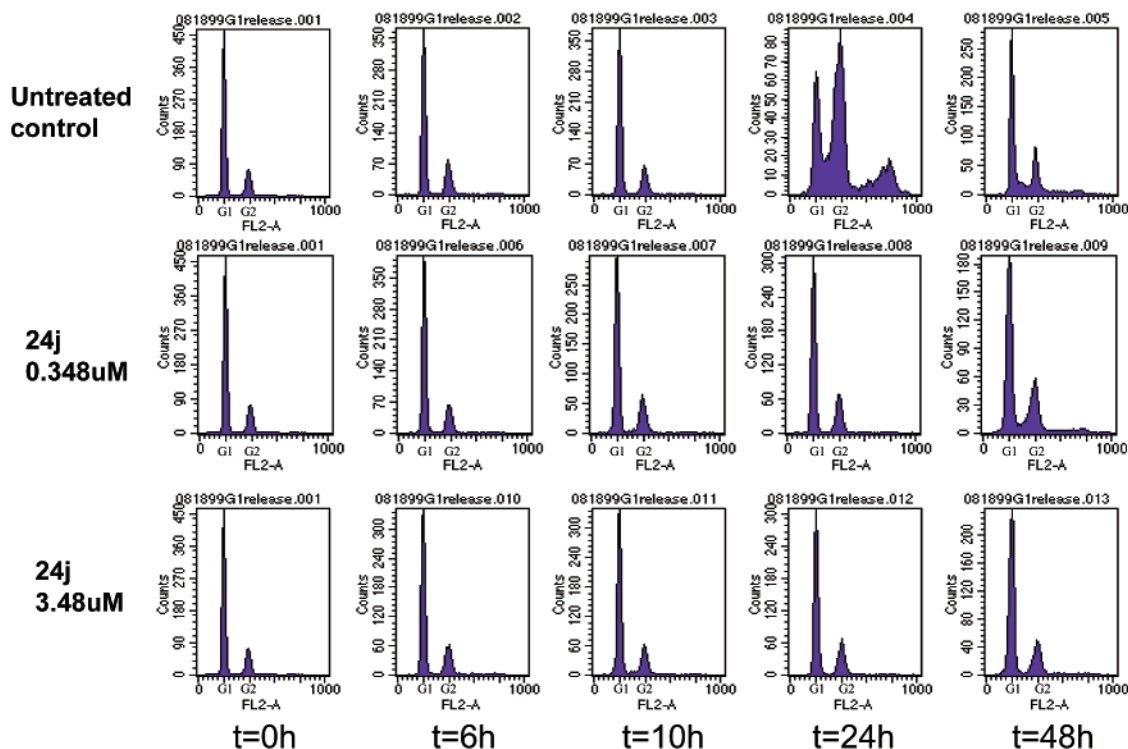


Figure 7. FACS diagram showing the effect of **24j** in G1-arrested AG1523.

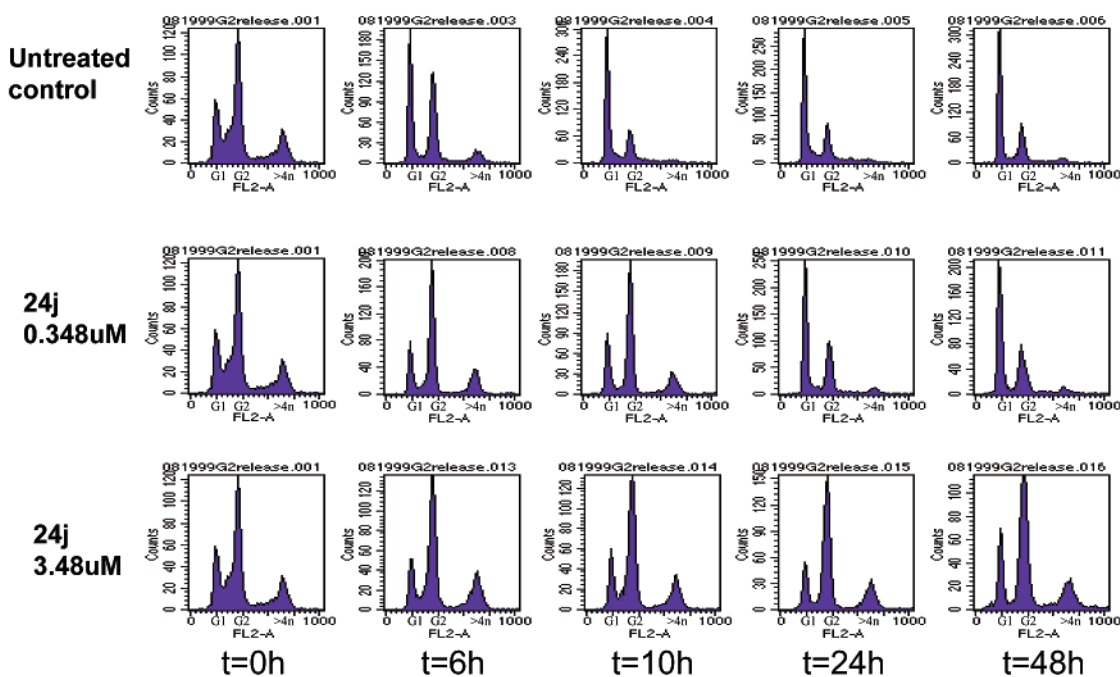


Figure 8. FACS diagram showing the effect of **24j** in G2-synchronized AG1523.

consistent with the *in vitro* potency of the compound on CDK2/E ($IC_{50} = 13$ nM).

Similarly, the ability of **24j** to impact cell cycle progression through G2/M was tested by exposing cells synchronized in G2/M to compound (Figure 8). When these G2/M-synchronized cells were exposed to vehicle alone, they progressed back into G1 within about 10 h. However, cells treated with 348 nM **24j** took longer (24–48 h) to progress into G1 indicative of a slowing through G2/M. Cells treated with 3.5 μ M **24j** remained completely blocked in G2/M. This result is biologically consistent with the activity of a compound able to inhibit

CDK1/B as indicated in its CDK inhibition profile (Table 9). The higher concentration of compound needed to completely block G2/M progression as compared to that needed to block exit from a G1 block may reflect the lower inhibitory potency of **24j** against CDK1/B (44 nM) as compared with that against CDK2/E (13 nM). When HCT116 cells were treated with **24j** and analyzed by FACS analysis, the appearance of a sub-G1 peak occurred within 24 h of treatment (data not shown).

HCT116 cells treated with **24j** appeared to lift off the culture plate and die. This observation, in combination with the appearance of a sub-G1 peak during FACS

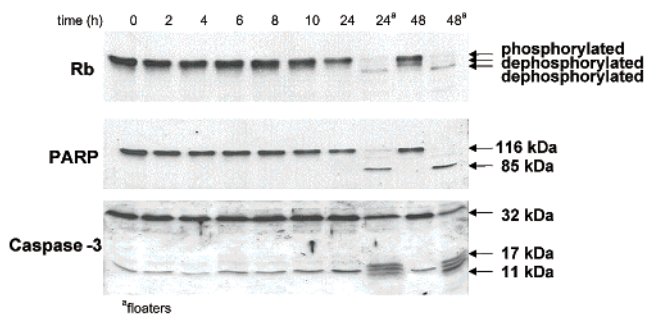


Figure 9. Compound **24j** induces apoptosis in asynchronous HCT116 tumor cells.

analysis, led us to examine the ability of **24j** to cause apoptosis in HCT116 cells in greater detail (Figure 9). HCT116 cells were treated with 580 nM **24j** and samples of attached cells, and floaters were taken as a function of time, harvested, and analyzed separately. After 24 h of **24j** treatment, inhibition of phosphorylation of the CDK substrate Rb was observed as would be predicted. This loss of phosphorylated Rb was observed predominantly in the floating population. Furthermore, these floating cells also contained the 85 kDa cleaved form of PARP and the 20 kDa and 11 kDa cleaved fragments of caspase 3. Cleavage of PARP and caspase 3 occurs as a result of activation of upstream proapoptotic caspases. Collectively, these results suggest that in HCT116 cells treated with **24j**, CDK inhibition results in inhibition of Rb phosphorylation and activation of the apoptotic machinery. This leads to detachment of the cells from the tissue culture dish and death. As judged by cleavage of apoptotic markers, significant death occurs within 24 h of treatment with **24j**. Cleavage of apoptotic markers did not occur when **24j** was evaluated in the normal human fibroblast, AG1523, under identical conditions (data not shown).

The likelihood that the biology of **24j** reflects CDK target inhibition was further examined by evaluating the activity of **24j** on arrested normal fibroblasts where cell cycle CDK activity is low or absent. Whereas **24j** had potent growth inhibitory activity on HCT116 cells reflecting cell cycle inhibition and death, it lacked activity in arrested fibroblasts (Figure 10). This lack of activity is consistent with **24j** killing through a CDK inhibition mechanism.

Conclusion

We have made many new compounds that explored the structure–activity relationships (SAR) of the C3 position of our indenopyrazole series of CDK inhibitors. We have shown that C3 can be substituted with heterocycles and alkyls in addition to other phenyl groups. A crystal structure was determined, which identifies interactions necessary for good inhibition. As expected, these compounds bind in the ATP pocket. Compound **24j** was found to be a unique inhibitor with cell cycle effects expected from inhibitors of this type. In addition, **24j** was found to be active in a variety of cancer cell lines. These data coupled with the inactivity in the normal cell line would suggest that compounds with this profile would provide an advantageous therapeutic window in vivo. The structural information and SAR data will allow us to continue to generate CDK inhibitors with better biological profiles.

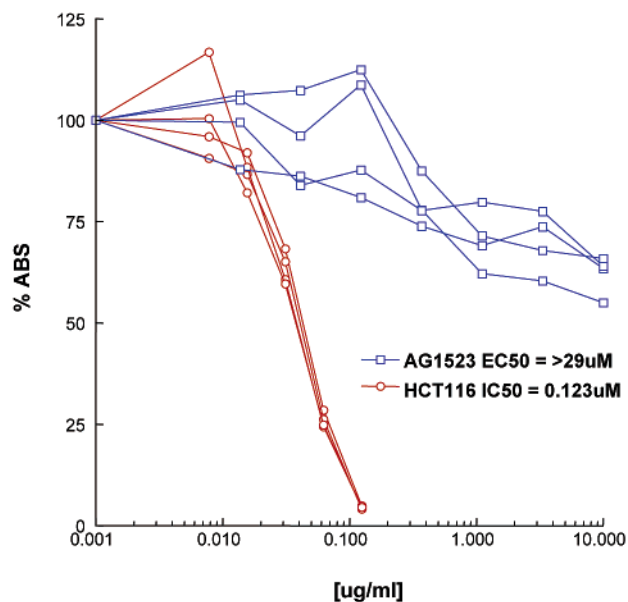


Figure 10. Graph of arrested AG1523 vs proliferating HCT116 for **24j**.

Experimental Section

All reactions were run under an atmosphere of dry nitrogen. All solvents were used without purification as acquired from commercial sources. NMR spectra were obtained using either a Varian (Palo Alto, CA) Unity-300, Inova-300, VXR-400, or Inova-400 spectrometer. Chemical shifts are reported in parts per million relative to tetramethylsilane (TMS) as internal standard. Microanalyses were performed by Quantitative Technologies Inc. and were within 0.4% of the calculated values. For compounds where microanalysis was not obtained, high-performance liquid chromatography (HPLC) purity was determined to be >98%. Mass spectra were obtained using either a Finnigan MAT8230 sector or MAT95S sector with API interface system. Flash chromatography was done using EM Science silica gel 60. HPLC purifications were performed on a Rainin Dynamax SD300 instrument using a C18 reverse phase column with acetonitrile/water (containing 0.05% trifluoroacetic acid (TFA)) as a mobile phase. HPLC purity values were obtained using a Rainin Dynamax SD300 instrument system with a photodiode array detector. Melting points were determined in open glass capillaries using a Thomas-Hoover UniMelt melting point apparatus and are uncorrected. Solubilities were determined by HPLC analysis of supernatants from a pH 7.4, 0.05 M potassium phosphate buffer-based assay.

CDK4/D1 Enzyme Inhibition. CDK4/D1 complexes were expressed in insect cells following dual infection by baculovirus vectors containing each of the components, and extracts of these cells were then prepared as described previously.²⁹ CDK4/D1 kinase activity was measured in 96 well polypropylene microtiter plates using a GST-60 kDa Rb fusion protein (comprising amino acids 378 to 928 of Rb) and γ -³²P-ATP and capturing the ³²P-labeled reaction products on GSH-Sepharose beads.³⁰ Briefly, each reaction (50 μ L) contained 50 mM Tris-HCl (pH 7.6), 10 mM MgCl₂, 10% dimethyl sulfoxide (DMSO), 1 mM dithiothreitol (DTT), 50 μ M ATP, 10 μ g/mL bovine serum albumin (BSA), 1% glycerol, 6 μ g GST-Rb (60 kDa Rb), and 0.5 μ Ci [γ -³²P]ATP. Kinase reactions were initiated by addition of 4 units of CDK4/D1. One unit of CDK4/D1 kinase activity results in the transfer of 1 pmol of ³²P per minute at room temperature to the GST-Rb fusion protein. After 15 min, 50 μ L of stop buffer (phosphate-buffered saline (PBS) with 100 mM Na₂EDTA, 10 mM ATP, 200 μ g/mL BSA, and 0.2% NP-40) was added to the reaction. Half of the reaction was then transferred to a Millipore MHVB N45 filter plate containing 50 μ L GSH-Sepharose beads (25% slurry in PBS with 0.8% NP40 and 80 mM Na₂EDTA) to capture the GST-Rb. The plates were incubated at room temperature for 90 min with

continuous mixing on a plate shaker. After they were filtered, each well was washed 5 times with 200 μ L of PBS containing 0.5% NP-40. The samples were dried, and 50 μ L of Microscint scintillation fluid was added to each well. The 32 P radioactivity in each sample was determined using the Packard Top Count scintillation counter. In a typical experiment, less than 10% of the GST-Rb was phosphorylated and greater than 95% of the radioactivity was found in Rb by sodium dodecyl sulfate (SDS)–PAGE analysis.

CDK2/E Enzyme Inhibition. CDK2/his-cyclinE was prepared as previously described.³¹ CDK2/E kinase reactions were carried out in 50 μ L reactions containing 50 mM Tris-HCl (pH 7.6), 10 mM MgCl₂, 10% DMSO, 1 mM DTT, 50 μ M ATP, 0.05 μ Ci [γ - 32 P]ATP (2000 Ci/mmol, NEN Life Science Products), and 6 μ M GST-Rb fusion. After they were incubated at room temperature, the reactions were terminated by addition of an equal volume of cold PBS containing 100 mM ethylenediaminetetraacetic acid (EDTA), 10 mM ATP, 200 μ g/mL BSA, and 0.2% NP40. Aliquots of the stopped reactions were processed as described previously.³⁰

Purification and Crystallization of Human CDK2. CDK2 protein was prepared and purified as previously described³² except for the addition of 10% (v/v) glycerol during the SP-sepharose and ATP-agarose column steps. Protein was concentrated to 6 mg/mL using a Collodion concentrator against 10 mM HEPES, pH 7.4, 15 mM NaCl. Crystals were grown at 18 °C from sitting drops containing premixed and filtered solutions of 3.0 mg/mL CDK2, 32.5 mM HEPES, pH 7.4, 11.3 mM sodium chloride, 12.5 mM ammonium acetate, 2 mM DTT, and 2–4% PEG 4000 against 100 mM HEPES, pH 7.4, 50 mM ammonium acetate, 2 mM DTT, and 4–14% PEG 4000. Crystals appeared in 1 day and grew for 1 week to approximately 0.25 mm \times 0.25 mm in size.

Crystal Preparation, Data Collection, and Processing. To prevent the crystals from cracking when soaked with inhibitor, CDK2 crystals were cross-linked in a solution of 0.1% glutaraldehyde, 10 mM sodium phosphate, pH 7.5, and 15 mM sodium chloride for 30 min. The cross-linked crystals were soaked for 6 days in inhibitor solution (0.5 mM **13q**, 0.5% DMSO, 10 mM HEPES, pH 7.4, 15 mM sodium chloride) and then briefly transferred into cryo-protectant (10 mM HEPES, pH 7.4, 15 mM sodium chloride, 25% MPD) and flash frozen in liquid nitrogen. Data were collected at the DND-CAT beam line, Advanced Photon Source, Argonne National Laboratories. Data were processed, scaled, and merged with the program HKL.³³

Structure Solution and Refinement. Molecular replacement using the program EPMR³⁴ was used to generate an initial phasing model from a previously determined in-house structure of CDK2. After five cycles of refinement (positional refinement, simulated annealing, and B-factor refinement) using the program CNX,³⁵ the electron density maps clearly showed the location of inhibitor inside the ATP binding site. Iterative cycles of refinement and model building were performed resulting in a final model, which includes residues 1–35, 43–147, 163–298, **13q**, and 104 water molecules. Data and refinement statistics are presented in Table 10.

Cellular Growth Inhibition Assays. Effects of compounds on growth of the following transformed cell lines was evaluated; HCT116 (human colon carcinoma, ATCC), NCI-H460 (human lung carcinoma, ATCC), PC-3 (human prostate adenocarcinoma, ATCC), MiaPaCa-2 (human pancreatic carcinoma, ATCC), HT-29 (human colon adenocarcinoma, ATCC), HT-1080 (human colon fibrosarcoma, ATCC) and B16-F0 (murine melanoma, ATCC). In addition, death effects on normal human fibroblasts (AG1523; Coriell Institute for Medical Research) were evaluated in a colorimetric assay using sulforhodamine B (SRB).³⁶ Briefly, exponentially growing cells were seeded in wells of a 96 well microtiter plate at a concentration to allow for 3–5 doublings before obtaining 85% confluence (transformed cell lines) or at a concentration resulting in confluence and contact inhibition of growth (AG1523). Eighteen hours later, graded concentrations of test compounds were added to the cell plates. Plates were incu-

Table 10. Crystallographic Statistics for CDK2/**13q**

space group	P2 ₁ 2 ₁ 2 ₁
cell dimensions (Å)	<i>a</i> = 71.98, <i>b</i> = 72.20, <i>c</i> = 53.52
maximal resolution (Å)	1.70
total observations	329,259
unique reflections	31,367
completeness (%)	99.9
<i>R</i> _{merge} ^a	0.065
mean <i>I</i> / σ (<i>I</i>)	27.1
refinement resolution (Å)	20.0–1.85
<i>R</i> _{factor} ^b	0.212
<i>R</i> _{free} ^c	0.256
avg protein temp factor (Å)	31.1
avg inhibitor temp factor (Å)	40.5
rms bonds (Å)	0.0067
rms angles (°)	1.60

^a $R_{\text{merge}} = \sum_h \sum_j |I_{hj} - \bar{I}_h| / \sum_h \sum_j I_{hj}$, where I_{hj} is the j th observation of reflection h . ^b $R_{\text{factor}} = \sum_h |F_{\text{obs}} - |F_{\text{calc}}|| / \sum_h |F_{\text{obs}}|$, where F_{obs} and F_{calc} are the observed and the calculated structure factor amplitudes, respectively, for reflection h . ^c $R_{\text{free}} = R_{\text{factor}}$ for a 9.2% subset of reflections not used in the refinement.

bated for 5 (HCT116, NCI-H460, PC-3, MiaPaCa-s, HT-29, HT-1080, and B16-F0) or 6 (AG1523) days at 37 °C in 5% CO₂. A 50 μ L amount of cold 50% TCA was gently added to each well, and plates were placed at 4 °C for 1 h. Plates were decanted, rinsed 5 times with cold tap water, and allowed to air dry. A 50 μ L amount of 0.4% SRB in 1% acetic acid was added, and the plates were incubated at room temperature for 15 min. Plates were washed four times with 1% acetic acid and again allowed to air-dry. A 150 μ L amount of 10 mM Tris base was added, and plates were agitated on a plate shaker for 5 min before reading optical densities at 570 nm using a BIORAD 3550 plate reader.

Cell Cycle Analysis. Normal human fibroblasts derived from human foreskin (AG1523) were grown to confluence and maintained at confluence for a minimum of 5 days. Cells were trypsinized and subcultured at 8000 cells/cm² in growth medium containing 10% fetal calf serum, and the indicated concentrations of compound were added either immediately (G1 release) or 24 h later (G2 synchronized). Cells were incubated in the presence of compound for up to 48 h, and samples were harvested at the indicated time points after compound addition. Cells were trypsinized and fixed in ice cold ethanol for a minimum of 24 h. After ethanol was removed, RnaseA (Sigma Chemicals) was added at 180 μ g/mL for 30 min at room temperature followed by the addition of propidium iodide (Sigma Chemicals) at a final concentration of 50 μ g/mL. Samples were run on a Becton Dickinson FACScan flow cytometer equipped with a 488 nm argon-ion laser and analyzed using CELLQUEST software.

Western Blot Analysis. Asynchronous subconfluent HCT116 or AG1523 cells were treated with compound or vehicle control as indicated. Samples were taken at the indicated time points with attached cells and floaters harvested separately. Floaters, when present, were obtained by collection of the culture medium, washing of the monolayers, and centrifugation of the pooled medium and wash at 1000 rpm. Cells were processed by lysing in an SDS-based buffer containing phosphatase and proteinase cocktails and subjected to analysis by SDS gel electrophoresis on appropriate (7.5 or 10% depending on protein to be detected) polyacrylamide gels. Gel loading was normalized for total protein as determined by BioRad's DC protein analysis kit, and 5 μ g of protein was loaded per lane. Gels were blotted onto nitrocellulose membranes. Membranes were probed with the following antibodies: retinoblastoma (pRb14001A, Pharmingen); poly-ADP ribose polymerase (PARP 8192-1, Clontech); and caspase 3 65906E (Pharmingen). The presence of bound antibody was detected using the following enhanced chemiluminescence procedure as follows: a species specific secondary antibody conjugated to biotin was allowed to react with blots previously probed with protein specific primary antibodies. After extensive washes, blots were incubated with biotinylated horseradish peroxidase (HRP) and avidin (Vector Laboratories Vectastain

ABC Kit). Following extensive washes, the HRP substrate luminol (NEN Renaissance reagent) was added and allowed to react for 1 min. Membranes were lightly hand-blotted dry, exposed to Kodak X-OMAT Blue autoradiography film, and developed.

Compounds **5a–m** and **8a–h** were prepared as illustrated in Scheme 1 using the procedures as previously described¹⁹ with the appropriate starting materials and reagents.

3-Phenyl-5-(acetamido)indeno[1,2-*c*]pyrazol-4-one (5a). mp >300 °C. ¹H NMR (300 MHz, DMSO-*d*₆): δ 10.18 (s, 1 H), 8.25–8.21 (m, 3 H), 7.61–7.49 (m, 4 H), 7.23 (d, *J* = 7.0 Hz, 1 H), 2.20 (s, 3 H). HRMS (CI) calcd for C₁₈H₁₄N₃O₂ (M + H)⁺, 304.1086; found, 304.1065. Anal. (C₁₈H₁₃N₃O₂·0.25H₂O) C, H, N.

3-(4-Methylphenyl)-5-(acetamido)indeno[1,2-*c*]pyrazol-4-one (5b). mp >300 °C. ¹H NMR (300 MHz, DMSO-*d*₆): δ 13.78 (s, 1 H), 10.18 (s, 1 H), 8.23 (d, *J* = 8.8 Hz, 1 H), 8.11 (d, *J* = 8.1 Hz, 2 H), 7.50 (dd, *J* = 8.0, 7.7 Hz, 1 H), 7.39 (d, *J* = 8.1 Hz, 2 H), 7.22 (d, *J* = 7.3 Hz, 1 H), 2.39 (s, 3 H), 2.20 (s, 3 H). HRMS (CI) calcd for C₁₉H₁₆N₃O₂ (M + H)⁺, 318.1243; found, 318.1222. Anal. (C₁₉H₁₅N₃O₂) C, H, N.

3-(4-Ethylphenyl)-5-(acetamido)indeno[1,2-*c*]pyrazol-4-one (5c). mp 292–294 °C. ¹H NMR (300 MHz, DMSO-*d*₆): δ 10.19 (s, 1 H), 8.24 (d, *J* = 8.5 Hz, 1 H), 8.14 (d, *J* = 8.0 Hz, 2 H), 7.51 (t, *J* = 8.5 Hz, 1 H), 7.43 (d, *J* = 8.0 Hz, 2 H), 7.23 (d, *J* = 8.5 Hz, 1 H), 2.69 (q, *J* = 7.0 Hz, 2 H), 2.20 (s, 3 H), 1.22 (t, *J* = 7.0 Hz, 3 H). HRMS (CI) calcd for C₂₀H₁₈N₃O₂ (M + H)⁺, 332.1399; found, 332.1388. Anal. (C₂₀H₁₇N₃O₂·0.18H₂NNH₂) C, H, N.

3-(4-*n*-Propylphenyl)-5-(acetamido)indeno[1,2-*c*]pyrazol-4-one (5d). mp 266–269 °C. ¹H NMR (300 MHz, DMSO-*d*₆): δ 10.19 (s, 1 H), 8.24 (d, *J* = 8.5 Hz, 1 H), 8.13 (d, *J* = 8.0 Hz, 2 H), 7.51 (t, *J* = 8.5 Hz, 1 H), 7.42 (d, *J* = 8.0 Hz, 2 H), 7.23 (d, *J* = 8.5 Hz, 1 H), 2.63 (t, *J* = 7.5 Hz, 2 H), 2.20 (s, 3 H), 1.64 (sextet, *J* = 7.5 Hz, 2 H), 0.92 (t, *J* = 7.5 Hz, 3 H). HRMS (CI) calcd for C₂₁H₂₀N₃O₂ (M + H)⁺, 346.1556; found, 346.1555. Anal. (C₂₁H₁₉N₃O₂) C, H, N.

3-(4-*n*-Butylphenyl)-5-(acetamido)indeno[1,2-*c*]pyrazol-4-one (5e). mp 256–259 °C. ¹H NMR (300 MHz, DMSO-*d*₆): δ 13.80 (s, 1 H), 10.19 (s, 1 H), 8.23 (d, *J* = 8.5 Hz, 1 H), 8.13 (d, *J* = 8.0 Hz, 2 H), 7.51 (t, *J* = 8.5 Hz, 1 H), 7.42 (m, 3 H), 7.22 (d, *J* = 8.5 Hz, 1 H), 2.65 (t, *J* = 7.0 Hz, 2 H), 2.20 (s, 3 H), 1.59 (quintet, *J* = 7.0 Hz, 2 H), 1.33 (sextet, *J* = 7.0 Hz, 2 H), 0.91 (t, *J* = 7.0 Hz, 3 H). HRMS (CI) calcd for C₂₂H₂₂N₃O₂ (M + H)⁺, 360.1712; found, 360.1701.

3-(4-Hydroxyphenyl)-5-(acetamido)indeno[1,2-*c*]pyrazol-4-one (5f). mp 289 °C. ¹H NMR (300 MHz, DMSO-*d*₆): δ 13.60 (s, 1 H), 10.21 (s, 1 H), 8.24 (d, *J* = 8.4 Hz, 1 H), 8.09 (d, *J* = 8.8 Hz, 2 H), 7.51 (dd, *J* = 8.4, 7.3 Hz, 1 H), 7.23 (d, *J* = 7.0 Hz, 1 H), 6.95 (d, *J* = 8.8 Hz, 2 H), 6.55 (s, 1 H), 2.21 (s, 3 H). HRMS (CI) calcd for C₁₈H₁₄N₃O₃ (M + H)⁺, 320.1035; found, 320.1030. Anal. (C₁₈H₁₃N₃O₃) C, H, N.

3-(4-Ethoxyphenyl)-5-(acetamido)indeno[1,2-*c*]pyrazol-4-one (5h). mp 287–288 °C. ¹H NMR (300 MHz, DMSO-*d*₆): δ 10.21 (s, 1 H), 8.24 (d, *J* = 8.5 Hz, 1 H), 8.17 (d, *J* = 9.0 Hz, 2 H), 7.50 (t, *J* = 8.5 Hz, 1 H), 7.22 (d, *J* = 8.5 Hz, 1 H), 7.13 (d, *J* = 9.0 Hz, 2 H), 4.12 (q, *J* = 7.5 Hz, 2 H), 2.20 (s, 3 H), 1.37 (t, *J* = 7.5 Hz, 3 H). HRMS (CI) calcd for C₂₀H₁₈N₃O₃ (M + H)⁺, 348.1348; found, 348.1325. Anal. (C₂₀H₁₇N₃O₃) C, H, N.

3-(4-Phenoxyphenyl)-5-(acetamido)indeno[1,2-*c*]pyrazol-4-one (5i). mp >300 °C. ¹H NMR (300 MHz, DMSO-*d*₆): δ 10.18 (s, 1 H), 8.24 (m, 3 H), 7.54–7.43 (m, 3 H), 7.25–7.11 (m, 6 H), 2.19 (s, 3 H). HRMS (CI) calcd for C₂₄H₁₈N₃O₃ (M + H)⁺, 396.1348; found, 396.1320. Anal. (C₂₄H₁₇N₃O₃·0.25H₂O) C, H, N.

3-(4-(*N,N*-Dimethylamino)phenyl)-5-(acetamido)indeno[1,2-*c*]pyrazol-4-one (5j). mp >300 °C. ¹H NMR (300 MHz, DMSO-*d*₆): δ 10.28 (s, 1 H), 8.23 (d, *J* = 8.5 Hz, 1 H), 8.09 (d, *J* = 9.0 Hz, 2 H), 7.48 (t, *J* = 8.5 Hz, 1 H), 7.20 (d, *J* = 8.5 Hz,

1 H), 6.85 (d, *J* = 9.0 Hz, 2 H), 3.04 (s, 6 H), 2.20 (s, 3 H). HRMS (CI) calcd for C₂₀H₁₉N₄O₂ (M + H)⁺, 347.1508; found, 347.1496. Anal. (C₂₀H₁₈N₄O₂) C, H, N.

3-(4-Piperidinophenyl)-5-(acetamido)indeno[1,2-*c*]pyrazol-4-one (5k). mp 289–291 °C. ¹H NMR (300 MHz, DMSO-*d*₆): δ 10.26 (s, 1 H), 8.24 (d, *J* = 8.0 Hz, 1 H), 8.07 (d, *J* = 8.5 Hz, 2 H), 7.49 (t, *J* = 8.0 Hz, 1 H), 7.21 (d, *J* = 8.0 Hz, 1 H), 7.06 (d, *J* = 8.5 Hz, 2 H), 3.30 (m, 4 H), 2.20 (s, 3 H), 1.60 (m, 6 H). HRMS (CI) calcd for C₂₃H₂₃N₄O₂ (M + H)⁺, 387.1821; found, 387.1801. Anal. (C₂₃H₂₂N₄O₂) C, H, N.

3-(4-Morpholinophenyl)-5-(acetamido)indeno[1,2-*c*]pyrazol-4-one (5l). mp >300 °C. ¹H NMR (300 MHz, DMSO-*d*₆): δ 10.23 (s, 1 H), 8.24 (d, *J* = 9.0 Hz, 1 H), 8.11 (d, *J* = 9.0 Hz, 2 H), 7.49 (t, *J* = 9.0 Hz, 1 H), 7.21 (d, *J* = 9.0 Hz, 1 H), 7.10 (d, *J* = 9.0 Hz, 2 H), 3.76 (m, 4 H), 3.27 (m, 4 H), 2.20 (s, 3 H). HRMS (CI) calcd for C₂₂H₂₁N₄O₃ (M + H)⁺, 389.1614; found, 389.1607. Anal. (C₂₂H₂₀N₄O₃) C, H, N.

3-(4-Methylthiophenyl)-5-(acetamido)indeno[1,2-*c*]pyrazol-4-one (5m). mp 280–283 °C. ¹H NMR (300 MHz, DMSO-*d*₆): δ 10.21 (s, 1 H), 8.22 (d, *J* = 8.5 Hz, 1 H), 8.15 (d, *J* = 8.5 Hz, 2 H), 7.49 (t, *J* = 8.5 Hz, 1 H), 7.44 (d, *J* = 8.5 Hz, 2 H), 7.20 (d, *J* = 8.5 Hz, 1 H), 2.55 (s, 3 H), 2.20 (s, 3 H). HRMS (CI) calcd for C₁₉H₁₆N₃O₂S (M + H)⁺, 350.0963; found, 350.0956. Anal. (C₁₉H₁₅N₃O₂S) C, H, N.

3-(4-(*N,N*-Dimethylamino)phenyl)-5-(morpholinoacetamido)indeno[1,2-*c*]pyrazol-4-one (8a). mp >300 °C. ¹H NMR (300 MHz, DMSO-*d*₆): δ 11.56 (s, 1 H), 8.41 (d, *J* = 8.5 Hz, 1 H), 8.08 (d, *J* = 9.0 Hz, 2 H), 7.49 (t, *J* = 8.5 Hz, 1 H), 7.22 (d, *J* = 8.5 Hz, 1 H), 6.85 (d, *J* = 9.0 Hz, 2 H), 3.82 (m, 4 H), 3.21 (s, 2 H), 3.03 (s, 6 H), 2.59 (m, 4 H). HRMS (ESI) calcd for C₂₄H₂₆N₅O₃ (M + H)⁺, 432.2036; found, 432.2020. Anal. (C₂₄H₂₅N₅O₃·1.0TFA) C, H, N.

3-(4-(*N,N*-Dimethylamino)phenyl)-5-(4-hydroxypiperidinoacetamido)indeno[1,2-*c*]pyrazol-4-one (8b). mp 264–267 °C. ¹H NMR (300 MHz, DMSO-*d*₆): δ 11.52 (s, 1 H), 8.40 (d, *J* = 8.0 Hz, 1 H), 8.08 (d, *J* = 9.0 Hz, 2 H), 7.49 (t, *J* = 8.0 Hz, 1 H), 7.21 (d, *J* = 8.0 Hz, 1 H), 6.83 (d, *J* = 9.0 Hz, 2 H), 3.60 (m, 1 H), 3.16 (s, 2 H), 3.02 (s, 6 H), 2.80 (m, 2 H), 2.36 (m, 2 H), 1.83 (m, 2 H), 1.68 (m, 2 H). HRMS (ESI) calcd for C₂₅H₂₈N₅O₃ (M + H)⁺, 446.2192; found, 446.2206. Anal. (C₂₅H₂₇N₅O₃) C, H, N.

3-(4-(*N,N*-Dimethylamino)phenyl)-5-(4-(aminomethyl)piperidinoacetamido)indeno[1,2-*c*]pyrazol-4-one (8c). ¹H NMR (300 MHz, DMSO-*d*₆): δ 11.74 (s, 1 H), 8.38 (d, *J* = 8.0 Hz, 1 H), 8.10 (d, *J* = 9.0 Hz, 2 H), 7.48 (t, *J* = 8.0 Hz, 1 H), 7.19 (d, *J* = 8.0 Hz, 1 H), 6.80 (d, *J* = 9.0 Hz, 2 H), 3.15 (s, 2 H), 3.02 (s, 6 H), 2.87 (m, 2 H), 2.59 (d, *J* = 6.5 Hz, 2 H), 2.23 (m, 2 H), 1.71 (m, 2 H), 1.63–1.54 (m, 2 H), 1.33 (m, 1 H). HRMS (ESI) calcd for C₂₆H₃₁N₆O₂ (M + H)⁺, 459.2508; found, 459.2508.

3-(4-(*N,N*-Dimethylamino)phenyl)-5-((4-methylpiperazino)acetamido)indeno[1,2-*c*]pyrazol-4-one (8d). mp >300 °C. ¹H NMR (300 MHz, DMSO-*d*₆): δ 11.65 (s, 1 H), 8.40 (d, *J* = 8.0 Hz, 1 H), 8.13 (d, *J* = 9.0 Hz, 2 H), 7.49 (t, *J* = 8.0 Hz, 1 H), 7.21 (d, *J* = 8.0 Hz, 1 H), 6.81 (d, *J* = 9.0 Hz, 2 H), 3.18 (s, 2 H), 3.02 (s, 6 H), 2.57 (m, 8 H), 2.28 (s, 3 H). HRMS (ESI) calcd for C₂₅H₂₉N₆O₂ (M + H)⁺, 445.2352; found, 445.2359. Anal. (C₂₅H₂₈N₆O₂·0.25H₂O) C, H, N.

3-(4-Morpholinophenyl)-5-(morpholinoacetamido)indeno[1,2-*c*]pyrazol-4-one (8e). mp 257–258 °C. ¹H NMR (300 MHz, DMSO-*d*₆): δ 11.56 (s, 1 H), 8.40 (d, *J* = 8.0 Hz, 1 H), 8.11 (d, *J* = 9.0 Hz, 2 H), 7.50 (t, *J* = 8.0 Hz, 1 H), 7.22 (d, *J* = 8.0 Hz, 1 H), 7.11 (d, *J* = 9.0 Hz, 2 H), 3.82 (m, 4 H), 3.75 (m, 4 H), 3.29 (m, 4 H), 3.20 (s, 2 H), 2.59 (m, 4 H). HRMS (ESI) calcd for C₂₆H₂₈N₅O₄ (M + H)⁺, 474.2141; found, 474.2151.

3-(4-Morpholinophenyl)-5-(4-hydroxypiperidinoacetamido)indeno[1,2-*c*]pyrazol-4-one (8f). mp 241–245 °C. ¹H NMR (300 MHz, DMSO-*d*₆): δ 11.52 (s, 1 H), 8.41 (d, *J* = 8.5 Hz, 1 H), 8.11 (d, *J* = 9.0 Hz, 2 H), 7.50 (t, *J* = 8.5 Hz, 1 H), 7.22 (d, *J* = 8.5 Hz, 1 H), 7.09 (d, *J* = 9.0 Hz, 2 H), 3.77 (m, 4 H), 3.60 (m, 1 H), 3.28 (m, 4 H), 3.16 (s, 2 H), 2.80 (m, 2 H), 2.33 (m, 2 H), 1.84 (m, 2 H), 1.70 (m, 2 H). HRMS (ESI) calcd for C₂₇H₃₀N₅O₄ (M + H)⁺, 488.2298; found, 488.2290. Anal. (C₂₇H₂₉N₅O₄·0.25H₂O) C, H, N.

3-(4-Morpholinophenyl)-5-(4-(aminomethyl)piperidinoacetamido)indeno[1,2-*c*]pyrazol-4-one (8g). mp 237–240 °C. ¹H NMR (300 MHz, DMSO-*d*₆): δ 11.73 (s, 1 H), 8.41 (d, *J* = 8.5 Hz, 1 H), 8.13 (d, *J* = 9.0 Hz, 2 H), 7.50 (t, *J* = 8.5 Hz, 1 H), 7.21 (d, *J* = 8.5 Hz, 1 H), 7.07 (d, *J* = 9.0 Hz, 2 H), 3.76 (m, 4 H), 3.27 (m, 4 H), 3.16 (s, 2 H), 2.89 (m, 2 H), 2.57 (d, *J* = 6.5 Hz, 2 H), 2.22 (m, 2 H), 1.70 (m, 2 H), 1.62–1.53 (m, 2 H), 1.31 (m, 1 H). HRMS (ESI) calcd for C₂₈H₃₃N₆O₃ (M + H)⁺, 501.2614; found, 501.2619.

3-(4-Morpholinophenyl)-5-(4-methylpiperazino)acetamidoindeno[1,2-*c*]pyrazol-4-one (8h). mp 256–258 °C. ¹H NMR (300 MHz, DMSO-*d*₆): δ 13.53 (brs, 1 H), 11.60 (s, 1 H), 8.41 (d, *J* = 8.5 Hz, 1 H), 8.15 (d, *J* = 9.0 Hz, 2 H), 7.50 (t, *J* = 8.5 Hz, 1 H), 7.22 (d, *J* = 8.5 Hz, 1 H), 7.08 (d, *J* = 9.0 Hz, 2 H), 3.76 (m, 4 H), 3.27 (m, 4 H), 3.18 (s, 2 H), 2.57 (m, 8 H), 2.27 (s, 3 H). HRMS (ESI) calcd for C₂₇H₃₁N₆O₃ (M + H)⁺, 487.2458; found, 487.2447.

2-Acetyl-4-nitro-1*H*-indene-1,3(2*H*)-dione (10a). A solution of 3-nitrophthalic anhydride (4.2 g, 20 mmol) and 2,4-pentanedione (2.0 mL, 20 mmol) in acetic anhydride (11.3 mL, 120 mmol) at 25 °C was treated dropwise with triethylamine (5.6 mL, 40 mmol). The reaction mixture was stirred at 25 °C for 30 min and quenched with 1 M HCl (45 mL). The solid that precipitated was filtered and washed with ether (2 × 25 mL) and hexane (3 × 25 mL) to give the nitrotrione **10a** (3.7 g, 80%) as a brown solid; mp 144–145 °C. ¹H NMR (300 MHz, DMSO-*d*₆): δ 8.05 (dd, *J* = 7.0, 1.5 Hz, 1 H), 7.96–7.87 (m, 2 H), 2.49 (s, 3 H). HRMS (CI) calcd for C₁₁H₈N₂O₅ (M + H)⁺, 234.0402; found, 234.0395. Anal. (C₁₁H₇NO₅) C, H, N.

2-Acetyl-4-amino-1*H*-indene-1,3(2*H*)-dione (11a). A solution of **10a** (700 mg, 3.0 mmol), zinc dust (6.4 g, 99 mmol), and calcium chloride (220 mg, 2.0 mmol) in 4:1 ethanol/water (22 mL) was refluxed for 1.5 h. The reaction mixture was filtered hot over Celite and washed with hot 4:1 ethanol/water (50 mL). The filtrate was concentrated in vacuo, the crude residue was dissolved in methanol (10 mL), and the solid was filtered. The filtrate was concentrated in vacuo, and the solid was triturated with ether (10 mL) and hexane (20 mL) to give the anilinetriene **11a** (500 mg, 82%) as an orange solid; mp >265 °C. ¹H NMR (300 MHz, DMSO-*d*₆): δ 7.22 (dd, *J* = 8.1, 7.3 Hz, 1 H), 6.75 (d, *J* = 8.1 Hz, 1 H), 6.68 (d, *J* = 6.9 Hz, 1 H), 6.29 (brs, 2 H), 2.31 (s, 3 H). HRMS (CI) calcd for C₁₁H₁₀NO₃ (M + H)⁺, 204.0661; found, 204.0685.

N-(2-Acetyl-1,3-dioxo-2,3-dihydro-1*H*-inden-4-yl)acetamide (12a). A solution of **11a** (450 mg, 2.2 mmol) in acetic anhydride (10 mL) was refluxed for 2 h. The reaction mixture was cooled to room temperature, and the solid was filtered. The filtrate was diluted with heptane and concentrated in vacuo to give the acetamide **12a** (390 mg, 72%) as a tan solid; mp >265 °C. ¹H NMR (300 MHz, DMSO-*d*₆): δ 10.72 (s, 1 H), 8.41 (d, *J* = 8.1 Hz, 1 H), 7.49 (dd, *J* = 8.1, 7.3 Hz, 1 H), 7.14 (d, *J* = 7.0 Hz, 1 H), 2.31 (s, 3 H), 2.18 (s, 3 H). HRMS (CI) calcd for C₁₃H₁₂NO₄ (M + H)⁺, 246.0766; found, 246.0758.

3-Methyl-5-(acetamido)indeno[1,2-*c*]pyrazol-4-one (13a). A solution of **12a** (300 mg, 1.2 mmol), hydrazine (77 μL, 2.4 mmol), and *p*-toluenesulfonic acid (12 mg, 60 μmol) in *n*-butanol (20 mL) was refluxed for 4.5 h. Additional hydrazine (19 μL, 0.6 mmol and 77 μL, 2.4 mmol) was added at 4 and 2 h, respectively. The reaction mixture was cooled and concentrated in vacuo to give a crude residue. Purification by reverse phase HPLC gave the indenopyrazole **13a** (19 mg, 6%) as a tan solid; mp >250 °C. ¹H NMR (400 MHz, DMSO-*d*₆, 30 °C): δ 13.06 (brs, 1 H), 10.08 (s, 1 H), 8.16 (d, *J* = 8.3 Hz, 1 H), 7.44 (dd, *J* = 8.5, 7.3 Hz, 1 H), 7.12 (d, *J* = 7.3 Hz, 1 H), 2.33 (s, 3 H), 2.15 (s, 3 H). HRMS (CI) calcd for C₁₃H₁₂N₃O₂ (M + H)⁺, 242.0930; found, 242.0928. Anal. (C₁₃H₁₁N₃O₂·1.0TFA) C, H, N.

Compounds **13b–i,r–w** were prepared as illustrated in Scheme 2 using the procedure described for **13a** using the appropriate starting materials and reagents. Compounds **13j–q** were prepared as illustrated in Scheme 2 using the procedures as previously described¹⁹ with the appropriate starting materials and reagents.

3-Ethyl-5-(acetamido)indeno[1,2-*c*]pyrazol-4-one (13b). mp 242–244 °C. ¹H NMR (300 MHz, DMSO-*d*₆): δ 13.1 (brs, 1 H), 10.10 (s, 1 H), 8.16 (d, *J* = 8.4 Hz, 1 H), 7.43 (dd, *J* = 7.9, 7.9 Hz, 1 H), 7.12 (d, *J* = 7.0 Hz, 1 H), 2.67 (q, *J* = 7.6 Hz, 2 H), 2.14 (s, 3 H), 1.29 (t, *J* = 7.7 Hz, 3 H). HRMS (ESI) calcd for C₁₄H₁₄N₃O₂ (M + H)⁺, 256.1086; found, 256.1090. Anal. (C₁₄H₁₃N₃O₂·0.5TFA) C, H, N.

3-*n*-Propyl-5-(acetamido)indeno[1,2-*c*]pyrazol-4-one (13c). mp 200–202 °C. ¹H NMR (300 MHz, DMSO-*d*₆): δ 13.12 (brs, 1 H), 10.11 (s, 1 H), 8.18 (d, *J* = 8.5 Hz, 1 H), 7.46 (dd, *J* = 8.4, 7.3 Hz, 1 H), 7.14 (d, *J* = 6.6 Hz, 1 H), 2.65 (t, *J* = 7.3 Hz, 2 H), 2.16 (s, 3 H), 1.78 (sextet, *J* = 7.5 Hz, 2 H), 0.92 (t, *J* = 7.5 Hz, 3 H). HRMS (CI) calcd for C₁₅H₁₆N₃O₂ (M + H)⁺, 270.1243; found, 270.1240. Anal. (C₁₅H₁₅N₃O₂·0.25TFA) C, H, N.

3-Isopropyl-5-(acetamido)indeno[1,2-*c*]pyrazol-4-one (13d). mp >250 °C. ¹H NMR (300 MHz, DMSO-*d*₆): δ 13.08 (s, 1 H), 10.10 (s, 1 H), 8.14 (d, *J* = 8.4 Hz, 1 H), 7.41 (dd, *J* = 8.5, 7.3 Hz, 1 H), 7.09 (d, *J* = 7.4 Hz, 1 H), 2.98 (septet, *J* = 6.9 Hz, 1 H), 2.12 (s, 3 H), 1.28 (d, *J* = 7.0 Hz, 6 H). HRMS (ESI) calcd for C₁₅H₁₆N₃O₂ (M + H)⁺, 270.1243; found, 270.1258. Anal. (C₁₅H₁₅N₃O₂·0.15H₂O) C, H, N.

2-Cyclopropylcarbonyl-4-nitro-1*H*-indene-1,3(2*H*)-dione (10e). A solution of sodium (2.3 g, 0.1 mol) in ethanol (200 mL) was treated dropwise with cyclopropyl methyl ketone (9.9 mL, 0.1 mol) and ethyl trifluoroacetate (11.9 mL, 0.1 mol). The reaction mixture was stirred at room temperature for 16 h, diluted with 1 M HCl (50 mL), and extracted with ethyl acetate. The organic extract was dried (MgSO₄), filtered, and concentrated in vacuo to give the dione **20e** (9.1 g, 50%) as a pale yellow oil. This was used without further purification. Dione **20e** (2.0 g, 11 mmol) was treated with the conditions described for the preparation of **10a** to give triene **10e** (2.1 g, 74%) as a bright yellow solid; mp 158–160 °C. ¹H NMR (300 MHz, DMSO-*d*₆): δ 7.80 (dd, *J* = 6.2, 2.6 Hz, 1 H), 7.73–7.69 (m, 2 H), 3.28–3.20 (m, 1 H), 0.88–0.84 (m, 2 H), 0.79–0.75 (m, 2 H). HRMS (CI) calcd for C₁₃H₁₀NO₅ (M + H)⁺, 260.0559; found, 260.0554.

3-Cyclopropyl-5-(acetamido)indeno[1,2-*c*]pyrazol-4-one (13e). mp 220–221 °C. ¹H NMR (300 MHz, DMSO-*d*₆): δ 13.20 (brs, 1 H), 10.05 (s, 1 H), 8.13 (d, *J* = 8.8 Hz, 1 H), 7.39 (dd, *J* = 8.5, 7.4 Hz, 1 H), 7.07 (d, *J* = 7.3 Hz, 1 H), 2.11 (s, 3 H), 1.94–1.90 (m, 1 H), 1.10 (d, *J* = 6.6 Hz, 4 H). HRMS (CI) calcd for C₁₅H₁₃N₃O₂ (M+), 267.1008; found, 267.1011. Anal. (C₁₅H₁₃N₃O₂·0.2TFA) C, H, N.

3-Isobutyl-5-(acetamido)indeno[1,2-*c*]pyrazol-4-one (13f). mp 209–211 °C. ¹H NMR (300 MHz, DMSO-*d*₆): δ 13.12 (brs, 1 H), 10.12 (s, 1 H), 8.18 (d, *J* = 8.4 Hz, 1 H), 7.46 (dd, *J* = 8.4, 7.7 Hz, 1 H), 7.14 (d, *J* = 7.0 Hz, 1 H), 2.55 (d, *J* = 7.4 Hz, 2 H), 2.19–2.11 (m, 1 H), 2.16 (s, 3 H), 0.91 (d, *J* = 6.6 Hz, 6 H). HRMS (ESI) calcd for C₁₆H₁₈N₃O₂ (M + H)⁺, 284.1399; found, 284.1413. Anal. (C₁₆H₁₇N₃O₂·0.25TFA) C, H, N.

3-*n*-Butyl-5-(acetamido)indeno[1,2-*c*]pyrazol-4-one (13g). mp 187–189 °C. ¹H NMR (300 MHz, DMSO-*d*₆): δ 13.10 (s, 1 H), 10.09 (s, 1 H), 8.16 (d, *J* = 8.8 Hz, 1 H), 7.43 (dd, *J* = 7.7, 7.7 Hz, 1 H), 7.11 (d, *J* = 7.4 Hz, 1 H), 2.65 (t, *J* = 7.7 Hz, 2 H), 2.14 (s, 3 H), 1.72 (quintet, *J* = 7.5 Hz, 2 H), 1.30 (sextet, *J* = 7.4 Hz, 2 H), 0.88 (t, *J* = 7.4 Hz, 3 H). HRMS (CI) calcd for C₁₆H₁₈N₃O₂ (M + H)⁺, 284.1399; found, 284.1398. Anal. (C₁₆H₁₇N₃O₂·1.0TFA) C, H, N.

3-*t*-Butyl-5-(acetamido)indeno[1,2-*c*]pyrazol-4-one (13h). mp 234–236 °C. ¹H NMR (300 MHz, DMSO-*d*₆): δ 12.98 (brs, 1 H), 10.12 (s, 1 H), 8.16 (d, *J* = 8.4 Hz, 1 H), 7.41 (dd, *J* = 8.4, 7.3 Hz, 1 H), 7.11 (d, *J* = 7.3 Hz, 1 H), 2.13 (s, 3 H), 1.33 (s, 9 H). HRMS (CI) calcd for C₁₆H₁₈N₃O₂ (M + H)⁺, 284.1399; found, 284.1395. Anal. (C₁₆H₁₇N₃O₂·1.0TFA) C, H, N.

3-Cyclohexyl-5-(acetamido)indeno[1,2-*c*]pyrazol-4-one (13i). mp >250 °C. ¹H NMR (300 MHz, DMSO-*d*₆): δ 13.07 (brs, 1 H), 10.11 (s, 1 H), 8.15 (d, *J* = 8.4 Hz, 1 H), 7.41 (dd, *J* = 8.8, 7.0 Hz, 1 H), 7.10 (d, *J* = 7.3 Hz, 1 H), 2.75–2.60 (m, 1 H), 2.13 (s, 3 H), 1.95–1.85 (m, 2 H), 1.80–1.50 (m, 5 H), 1.40–1.15 (m, 3 H). HRMS (ESI) calcd for C₁₈H₂₀N₃O₂ (M + H)⁺, 310.1566; found, 310.1564. Anal. (C₁₈H₁₉N₃O₂·1.0H₂O) C, H, N.

3-Methyl-8-nitroindeno[1,2-c]pyrazol-4-one (15). Method

A. A solution of **10a** (100 mg, 0.4 mmol), hydrazine (27 μ L, 0.9 mmol), and *p*-toluenesulfonic acid (4 mg, 22 μ mol) in ethanol (1 mL) was refluxed for 1 h. The reaction mixture was cooled to room temperature, and the solid was filtered and washed with cold ethanol (10 mL) to give the hydrazone **14** (75 mg, 71%) as an orange-yellow solid. $^1\text{H NMR}$ (300 MHz, DMSO- d_6): δ 7.87 (dd, $J = 6.2, 2.2$ Hz, 1 H), 7.77–7.71 (m, 2 H), 5.59 (s, 2 H), 2.52 (s, 3 H). A solution of hydrazone **14** (75 mg, 0.3 mmol) was treated with the conditions described for the preparation of **13a** to give **15** (46 mg, 68%) as a solid.

Method B. A solution of **10a** was treated with the conditions described for the preparation of **13a** to give **15**. mp 224–225 °C. $^1\text{H NMR}$ (300 MHz, DMSO- d_6): δ 13.41 (brs, 1 H), 8.16 (d, $J = 7.3$ Hz, 1 H), 7.83 (d, $J = 6.9$ Hz, 1 H), 7.55 (dd, $J = 8.1, 7.3$ Hz, 1 H), 2.36 (s, 3 H). HRMS (CI) calcd for $\text{C}_{11}\text{H}_8\text{N}_3\text{O}_3$ (M + H) $^+$, 230.0566; found, 230.0574. Anal. ($\text{C}_{11}\text{H}_7\text{N}_3\text{O}_3 \cdot 0.1\text{H}_2\text{O}$) C, H, N.

3-Methyl-8-aminoindeno[1,2-c]pyrazol-4-one (16). A solution of **15** was treated with the conditions described for the preparation of **11a** to give **16** as a solid; mp 186–187 °C. $^1\text{H NMR}$ (300 MHz, DMSO- d_6): δ 7.01 (dd, $J = 8.0, 7.4$ Hz, 1 H), 6.77 (d, $J = 7.7$ Hz, 1 H), 6.73 (d, $J = 7.3$ Hz, 1 H), 2.28 (s, 3 H). HRMS (ESI) calcd for $\text{C}_{11}\text{H}_{10}\text{N}_3\text{O}$ (M + H) $^+$, 200.0824; found, 200.0831.

3-Methyl-8-(acetamido)indeno[1,2-c]pyrazol-4-one (17). A solution of **16** (10 mg, 50 μ mol) in dioxane (1 mL) was treated with saturated sodium bicarbonate (1 drop) and acetyl chloride (1 drop) and stirred at room temperature for 1 h. The reaction mixture was concentrated in vacuo and purified by reverse phase HPLC to give the indenopyrazole **17** (5 mg, 42%) as a pale yellow solid; mp 239–241 °C. $^1\text{H NMR}$ (400 MHz, DMSO- d_6 , 30 °C): δ 13.03 (brs, 1 H), 9.18 (brs, 1 H), 7.79 (br s, 1 H), 7.31–7.26 (m, 2 H), 2.34 (s, 3 H), 2.10 (s, 3 H). HRMS (CI) calcd for $\text{C}_{13}\text{H}_{12}\text{N}_3\text{O}_2$ (M + H) $^+$, 242.0930; found, 242.0933.

3-Ethyl-5-((4-carbamoylpiperidino)acetamido)indeno[1,2-c]pyrazol-4-one (13j). mp 208–210 °C. $^1\text{H NMR}$ (400 MHz, DMSO- d_6 , 140 °C): δ 10.85 (s, 1 H), 8.20 (d, $J = 8.3$ Hz, 1 H), 7.45 (dd, $J = 8.5, 7.4$ Hz, 1 H), 7.16 (d, $J = 7.0$ Hz, 1 H), 6.57 (brs, 2 H), 4.09 (brs, 1 H), 3.58 (s, 2 H), 3.16 (d, $J = 10.7$ Hz, 2 H), 2.73 (q, $J = 7.6$ Hz, 2 H), 2.67–2.65 (m, 2 H), 2.31–2.25 (m, 1 H), 1.99–1.86 (m, 4 H), 1.34 (t, $J = 7.6$ Hz, 3 H). HRMS (ESI) calcd for $\text{C}_{20}\text{H}_{24}\text{N}_5\text{O}_3$ (M + H) $^+$, 382.1879; found, 382.1886. Anal. ($\text{C}_{20}\text{H}_{23}\text{N}_5\text{O}_3 \cdot 1.0\text{TFA}$) C, H, N.

3-Isopropyl-5-((4-carbamoylpiperidino)acetamido)indeno[1,2-c]pyrazol-4-one (13k). mp 213–215 °C. $^1\text{H NMR}$ (400 MHz, DMSO- d_6 , 30 °C): δ 13.04 (brs, 1 H), 11.34 (s, 1 H), 8.35 (d, $J = 8.5$ Hz, 1 H), 7.44 (dd, $J = 8.1, 7.5$ Hz, 1 H), 7.13 (d, $J = 7.3$ Hz, 1 H), 6.68 (brs, 2 H), 3.12 (s, 2 H), 3.07–3.00 (m, 1 H), 2.89–2.86 (m, 2 H), 2.21–2.16 (m, 2 H), 2.12–2.08 (m, 1 H), 1.89–1.79 (m, 2 H), 1.74–1.72 (m, 2 H), 1.31 (d, $J = 6.9$ Hz, 6 H). HRMS (ESI) calcd for $\text{C}_{21}\text{H}_{26}\text{N}_5\text{O}_3$ (M + H) $^+$, 396.2036; found, 396.2045. Anal. ($\text{C}_{21}\text{H}_{25}\text{N}_5\text{O}_3 \cdot 1.7\text{TFA}$) C, H, N.

3-Cyclopropyl-5-((4-carbamoylpiperidino)acetamido)indeno[1,2-c]pyrazol-4-one (13l). mp 178–180 °C. $^1\text{H NMR}$ (400 MHz, DMSO- d_6 , 120 °C): δ 10.92 (brs, 1 H), 8.21 (d, $J = 8.3$ Hz, 1 H), 7.44 (dd, $J = 8.3, 7.3$ Hz, 1 H), 7.14 (d, $J = 6.9$ Hz, 1 H), 6.62 (brs, 2 H), 3.60–3.42 (m, 2 H), 3.17–3.04 (m, 2 H), 2.68–2.51 (m, 2 H), 2.30–2.21 (m, 1 H), 2.03–1.97 (m, 1 H), 1.96–1.84 (m, 4 H), 1.19–1.01 (m, 4 H). HRMS (ESI) calcd for $\text{C}_{21}\text{H}_{24}\text{N}_5\text{O}_3$ (M + H) $^+$, 394.1879; found, 394.1876. Anal. ($\text{C}_{21}\text{H}_{23}\text{N}_5\text{O}_3 \cdot 1.0\text{TFA}$) C, H, N; calcd, 13.80; found, 14.51.

3-Cyclohexyl-5-((4-carbamoylpiperidino)acetamido)indeno[1,2-c]pyrazol-4-one (13m). mp 229–231 °C. $^1\text{H NMR}$ (400 MHz, DMSO- d_6 , 120 °C): δ 11.60 (brs, 1 H), 8.16 (d, $J = 8.3$ Hz, 1 H), 7.46 (dd, $J = 8.3, 7.3$ Hz, 1 H), 7.17 (d, $J = 7.1$ Hz, 1 H), 6.67 (brs, 2 H), 3.82–3.68 (m, 2 H), 3.31–3.18 (m, 2 H), 2.79–2.74 (m, 3 H), 2.38–2.26 (m, 1 H), 1.99–1.91 (m, 6 H), 1.82–1.78 (m, 2 H), 1.72–1.64 (m, 3 H), 1.41–1.30 (m, 3 H). HRMS (ESI) calcd for $\text{C}_{24}\text{H}_{30}\text{N}_5\text{O}_3$ (M + H) $^+$, 436.2356; found, 436.2349. Anal. ($\text{C}_{24}\text{H}_{29}\text{N}_5\text{O}_3 \cdot 1.25\text{TFA}$) C, H, N.

3-Ethyl-5-(4-(aminomethyl)piperidinoacetamido)indeno[1,2-c]pyrazol-4-one (13n). mp 174–176 °C. $^1\text{H NMR}$

(400 MHz, DMSO- d_6 , 120 °C): δ 11.14 (s, 1 H), 8.28 (d, $J = 8.6$ Hz, 1 H), 7.65 (brs, 2 H), 7.52 (dd, $J = 8.3, 7.3$ Hz, 1 H), 7.14 (d, $J = 7.1$ Hz, 1 H), 3.33 (s, 2 H), 3.00 (d, $J = 10.5$ Hz, 2 H), 2.78 (d, $J = 6.9$ Hz, 2 H), 2.72 (q, $J = 7.6$ Hz, 2 H), 2.44–2.40 (m, 2 H), 1.82 (d, $J = 13.4$ Hz, 2 H), 1.74–1.68 (m, 1 H), 1.61–1.51 (m, 2 H), 1.34 (t, $J = 7.6$ Hz, 3 H). HRMS (ESI) calcd for $\text{C}_{20}\text{H}_{26}\text{N}_5\text{O}_2$ (M + H) $^+$, 368.2086; found, 368.2078. Anal. ($\text{C}_{20}\text{H}_{25}\text{N}_5\text{O}_2 \cdot 2.0\text{TFA}$) C, H, N.

3-Isopropyl-5-(4-(aminomethyl)piperidinoacetamido)indeno[1,2-c]pyrazol-4-one (13o). mp 187–189 °C. $^1\text{H NMR}$ (400 MHz, DMSO- d_6 , 120 °C): δ 11.40 (s, 1 H), 8.33 (d, $J = 8.5$ Hz, 1 H), 7.42 (dd, $J = 8.6, 7.1$ Hz, 1 H), 7.11 (dd, $J = 7.3, 7.1$ Hz, 1 H), 3.12 (s, 2 H), 3.10–3.01 (m, 2 H), 2.90–2.85 (m, 2 H), 2.56 (d, $J = 6.4$ Hz, 2 H), 2.33–2.21 (m, 2 H), 1.75–1.65 (m, 2 H), 1.60–1.45 (m, 2 H), 1.36 (d, $J = 6.8$ Hz, 6 H). HRMS (ESI) calcd for $\text{C}_{21}\text{H}_{28}\text{N}_5\text{O}_2$ (M + H) $^+$, 382.2243; found, 382.2254. Anal. ($\text{C}_{21}\text{H}_{27}\text{N}_5\text{O}_2 \cdot 2.0\text{TFA}$) C, H, N.

3-Cyclopropyl-5-(4-(aminomethyl)piperidinoacetamido)indeno[1,2-c]pyrazol-4-one (13p). mp 138–140 °C. $^1\text{H NMR}$ (400 MHz, DMSO- d_6 , 120 °C): δ 11.24 (s, 1 H), 8.30 (d, $J = 8.5$ Hz, 1 H), 7.65 (brs, 2 H), 7.43 (dd, $J = 8.5, 7.3$ Hz, 1 H), 7.11 (d, $J = 7.1$ Hz, 1 H), 3.22 (s, 2 H), 2.95 (app. d, $J = 11.5$ Hz, 2 H), 2.79 (d, $J = 6.8$ Hz, 2 H), 2.35 (app. t, $J = 11.2$ Hz, 2 H), 2.05–1.95 (m, 1 H), 1.81 (app. d, $J = 14.2$ Hz, 2 H), 1.70–1.62 (m, 1 H), 1.59 (dd, $J = 11.4, 3.6$ Hz, 1 H), 1.53 (dd, $J = 10.9, 3.8$ Hz, 1 H), 1.20–1.05 (m, 4 H). HRMS (ESI) calcd for $\text{C}_{21}\text{H}_{26}\text{N}_5\text{O}_2$ (M + H) $^+$, 380.2086; found, 380.2079. Anal. ($\text{C}_{21}\text{H}_{25}\text{N}_5\text{O}_2 \cdot 2.0\text{TFA}$) C, H, N.

3-Cyclohexyl-5-(4-(aminomethyl)piperidinoacetamido)indeno[1,2-c]pyrazol-4-one (13q). mp 196–198 °C. $^1\text{H NMR}$ (400 MHz, DMSO- d_6 , 120 °C): δ 11.19 (s, 1 H), 8.26 (d, $J = 8.5$ Hz, 1 H), 7.83–7.63 (brs, 2 H), 7.44 (dd, $J = 8.5, 8.0$ Hz, 1 H), 7.13 (d, $J = 7.1$ Hz, 1 H), 3.38 (s, 2 H), 3.06–3.01 (m, 1 H), 2.79–2.75 (m, 2 H), 2.01–1.95 (m, 4 H), 1.85–1.78 (m, 4 H), 1.77–1.57 (m, 5 H), 1.51–1.29 (m, 6 H). HRMS (ESI) calcd for $\text{C}_{24}\text{H}_{32}\text{N}_5\text{O}_2$ (M + H) $^+$, 422.2556; found, 422.2540. Anal. ($\text{C}_{24}\text{H}_{31}\text{N}_5\text{O}_2 \cdot 1.0\text{TFA}$) C, H, N.

Phenyl 1,3-dioxo-2-propionyl-2,3-dihydro-1H-inden-4-ylcarbamate (22a). A solution of aniline **11b** (1.1 g, 5.1 mmol), made using the chemistry described for **10a** and **11a**, and sodium carbonate (2.2 g, 200 wt %) in acetone (20 mL) was treated with phenylchloroformate (0.76 mL, 6.1 mmol). The reaction mixture was stirred at 50 °C for 30 min, cooled to room temperature, and diluted with water (20 mL) and ethyl acetate (20 mL). The organic phase was dried (MgSO_4), filtered, and concentrated in vacuo to give a solid. Trituration of the solid with ether gave the carbamate **22a** (1.2 g, 71%) as a tan solid; mp 146–148 °C. $^1\text{H NMR}$ (300 MHz, DMSO- d_6): δ 10.06 (s, 1 H), 8.22 (d, $J = 8.1$ Hz, 1 H), 7.74 (dd, $J = 8.1, 7.7$ Hz, 1 H), 7.45–7.40 (m, 3 H), 7.29–7.24 (m, 3 H), 2.90 (q, $J = 7.7$ Hz, 2 H), 1.15 (t, $J = 7.5$ Hz, 3 H). HRMS (ESI) calcd for $\text{C}_{19}\text{H}_{16}\text{NO}_5$ (M + H) $^+$, 338.1028; found, *m/z* 338.1020.

N-(1,3-Dioxo-2-propionyl-2,3-dihydro-1H-inden-4-yl)-urea (23a). A solution of carbamate **22a** (340 mg, 1.0 mmol) and ammonium hydroxide (0.28 mL, 2.0 mmol) in methylsulfoxide (5 mL) was heated at 90 °C for 4 h. The reaction mixture was concentrated in vacuo to give a crude residue. Purification by flash column chromatography (silica, ethyl acetate:hexane 1:1) gave the urea **23a** (190 mg, 71%) as a light yellow solid; mp >250 °C. $^1\text{H NMR}$ (300 MHz, DMSO- d_6): δ 8.45 (d, $J = 8.5$ Hz, 0.6 H), 8.40 (d, $J = 8.5$ Hz, 0.4 H), 7.53–7.46 (m, 1 H), 7.12 (d, $J = 7.4$ Hz, 1 H), 6.72 (brs, 2 H), 2.89–2.80 (m, 2 H), 1.22–1.15 (m, 3 H).

3-Ethyl-5-(carbamoylamino)indeno[1,2-c]pyrazol-4-one (24a). Trione **23a** was treated with the conditions described for the preparation of **13a**; mp 250 °C. $^1\text{H NMR}$ (300 MHz, DMSO- d_6): δ 9.27 (s, 1 H), 8.19 (d, $J = 8.8$ Hz, 1 H), 7.35 (dd, $J = 8.7, 7.2$ Hz, 1 H), 6.97 (d, $J = 7.3$ Hz, 1 H), 6.75 (brs, 2 H), 2.79 (q, $J = 7.6$ Hz, 2 H), 1.33 (t, $J = 7.7$ Hz, 3 H). HRMS (CI) calcd for $\text{C}_{13}\text{H}_{13}\text{N}_4\text{O}_2$ (M + H) $^+$, 257.1039; found, 257.1033. Anal. ($\text{C}_{13}\text{H}_{12}\text{N}_4\text{O}_2$) C, H, N.

Compounds **24b–m** were prepared as illustrated in Scheme 4 using the procedure described for **24a** using the appropriate starting materials and reagents.

3-Isopropyl-5-(carbamoylamino)indeno[1,2-*c*]pyrazol-4-one (24b). mp >250 °C. ¹H NMR (300 MHz, DMSO-*d*₆): δ 13.00 (brs, 1 H), 9.27 (s, 1 H), 8.16 (d, *J* = 8.7 Hz, 1 H), 7.31 (dd, *J* = 8.8, 7.3 Hz, 1 H), 6.93 (d, *J* = 7.0 Hz, 1 H), 6.70 (brs, 2 H), 2.98 (quintet, *J* = 6.9 Hz, 1 H), 1.28 (d, *J* = 6.6 Hz, 6 H). HRMS (CI) calcd for C₁₄H₁₅N₄O₂ (M + H)⁺, 271.1195; found, 271.1196. Anal. (C₁₄H₁₄N₄O₂·0.5TFA) C, H, N: calcd, 17.12; found, 10.23.

3-Cyclopropyl-5-(carbamoylamino)indeno[1,2-*c*]pyrazol-4-one (24c). mp 252–253 °C. ¹H NMR (400 MHz, DMSO-*d*₆, 120 °C): δ 12.80 (brs, 1 H), 9.20 (s, 1 H), 8.14 (d, *J* = 8.6 Hz, 1 H), 7.31 (dd, *J* = 8.6, 7.4 Hz, 1 H), 6.93 (d, *J* = 7.2 Hz, 1 H), 6.31 (brs, 2 H), 2.01–1.94 (m, 1 H), 1.18–1.08 (m, 4 H). HRMS (CI) calcd for C₁₄H₁₂N₄O₂ (M)⁺, 268.0960; found, 268.0972. Anal. (C₁₄H₁₂N₄O₂·0.15TFA) C, H, N.

3-Cyclohexyl-5-(carbamoylamino)indeno[1,2-*c*]pyrazol-4-one (24d). mp 178–179 °C. ¹H NMR (300 MHz, DMSO-*d*₆): δ 12.98 (brs, 1 H), 9.30 (s, 1 H), 8.16 (d, *J* = 8.4 Hz, 1 H), 7.31 (dd, *J* = 8.5, 7.3 Hz, 1 H), 6.93 (d, *J* = 7.0 Hz, 1 H), 6.70 (brs, 2 H), 2.70–2.62 (m, 1 H), 1.95–1.88 (m, 2 H), 1.75–1.53 (m, 4 H), 1.36–1.10 (m, 4 H). HRMS (ESI) calcd for C₁₇H₁₉N₄O₂ (M + H)⁺, 311.1508; found, 311.1500. Anal. (C₁₇H₁₈N₄O₂·0.25TFA) C, H, N.

3-(Pyrid-3-yl)-5-(acetamido)indeno[1,2-*c*]pyrazol-4-one (13r). mp >300 °C. ¹H NMR (300 MHz, DMSO-*d*₆): δ 10.09 (s, 1 H), 9.34 (d, *J* = 1.8 Hz, 1 H), 8.66 (d, *J* = 4.7, 1.4 Hz, 1 H), 8.46 (ddd, *J* = 8.1, 8.1, 1.8 Hz, 1 H), 8.19 (d, *J* = 8.4 Hz, 1 H), 7.59 (dd, *J* = 8.0, 4.7 Hz, 1 H), 7.49 (dd, *J* = 8.5, 7.3 Hz, 1 H), 7.43 (d, *J* = 8.1 Hz, 0.5 H), 7.20 (d, *J* = 6.9 Hz, 1 H), 7.07 (d, *J* = 8.0 Hz, 0.5 H), 2.16 (s, 3 H). HRMS (CI) calcd for C₁₇H₁₃N₄O₂ (M + H)⁺, 305.1039; found, 305.1048. Anal. (C₁₇H₁₂N₄O₂) C, H, N.

3-(Pyrid-4-yl)-5-(acetamido)indeno[1,2-*c*]pyrazol-4-one (13s). mp >300 °C. ¹H NMR (300 MHz, DMSO-*d*₆): δ 10.08 (s, 1 H), 8.76 (dd, *J* = 4.6, 1.7 Hz, 2 H), 8.18 (d, *J* = 8.5 Hz, 1 H), 8.06 (dd, *J* = 4.6, 1.7 Hz, 2 H), 7.49 (dd, *J* = 8.4, 7.3 Hz, 1 H), 7.19 (d, *J* = 7.3 Hz, 1 H), 2.16 (s, 3 H). HRMS (CI) calcd for C₁₇H₁₃N₄O₂ (M + H)⁺, 305.1039; found, 305.1046. Anal. (C₁₇H₁₂N₄O₂) C, H, N.

3-(Thien-2-yl)-5-(acetamido)indeno[1,2-*c*]pyrazol-4-one (13t). mp >300 °C. ¹H NMR (300 MHz, DMSO-*d*₆): δ 10.13 (s, 1 H), 8.22 (d, *J* = 8.7 Hz, 1 H), 7.98 (d, *J* = 3.1 Hz, 1 H), 7.83 (d, *J* = 4.8 Hz, 1 H), 7.49 (dd, *J* = 8.1, 8.0 Hz, 1 H), 7.27 (m, 1 H), 7.20 (d, *J* = 7.0 Hz, 1 H), 2.07 (s, 3 H). HRMS (CI) calcd for C₁₆H₁₂N₃O₂S (M + H)⁺, 310.0650; found, 310.0641. Anal. (C₁₆H₁₁N₃O₂S) C, H, N.

3-(3-Methylthien-2-yl)-5-(acetamido)indeno[1,2-*c*]pyrazol-4-one (13u). mp 275 °C. ¹H NMR (300 MHz, DMSO-*d*₆): δ 13.45 (brs, 1 H), 10.06 (brs, 1 H), 8.19 (d, *J* = 8.5 Hz, 1 H), 7.72–7.68 (m, 1 H), 7.47 (dd, *J* = 8.4, 7.7 Hz, 1 H), 7.19 (d, *J* = 7.0 Hz, 1 H), 7.06 (d, *J* = 5.1 Hz, 1 H), 2.36 (s, 3 H), 2.14 (s, 3 H). HRMS (ESI) calcd for C₁₇H₁₄N₃O₂S (M + H)⁺, 324.0807; found, 324.0811.

3-(2,5-Dichlorothien-3-yl)-5-(acetamido)indeno[1,2-*c*]pyrazol-4-one (13v). ¹H NMR (300 MHz, DMSO-*d*₆): δ 13.68 (brs, 1 H), 10.08 (brs, 1 H), 8.25 (d, *J* = 8.7 Hz, 1 H), 7.68 (brs, 1 H), 7.54 (dd, *J* = 8.1, 7.6 Hz, 1 H), 7.27 (brs, 1 H), 2.21 (s, 3 H). HRMS (ESI) calcd for C₁₆H₈N₃O₂SCl₂ (M – H)⁺, 375.9714; found, 375.9698.

3-(Furan-2-yl)-5-(acetamido)indeno[1,2-*c*]pyrazol-4-one (13w). mp >300 °C. ¹H NMR (300 MHz, DMSO-*d*₆): δ 13.90 (s, 1 H), 10.11 (s, 1 H), 8.22 (d, *J* = 8.4 Hz, 1 H), 8.00 (s, 1 H), 7.50 (dd, *J* = 8.5, 7.3 Hz, 1 H), 7.29 (s, 1 H), 7.23 (d, *J* = 6.9 Hz, 1 H), 2.19 (s, 3 H). HRMS (CI) calcd for C₁₆H₁₂N₃O₃ (M + H)⁺, 294.0879; found, 294.0878. Anal. (C₁₆H₁₁N₃O₃·0.26TFA·0.34acetone·0.45H₂O) C, H, N.

3-(Thien-2-yl)-5-(carbamoylamino)indeno[1,2-*c*]pyrazol-4-one (24e). mp 214 °C. ¹H NMR (300 MHz, DMSO-*d*₆): δ 13.75 (brs, 1 H), 9.28 (brs, 1 H), 8.22 (d, *J* = 8.0 Hz, 1 H), 7.93 (dd, *J* = 3.7, 1.1 Hz, 1 H), 7.83–7.77 (m, 1 H), 7.37 (dd, *J* = 8.8, 8.8 Hz, 1 H), 7.25–7.20 (m, 1 H), 7.05–7.00 (m, 1 H), 6.77 (brs, 2 H). HRMS (ESI) calcd for C₁₅H₁₁N₄O₂S (M + H)⁺, 311.0603; found, 311.0611.

3-(3-Methylthien-2-yl)-5-(carbamoylamino)indeno[1,2-*c*]pyrazol-4-one (24f). mp 270 °C (dec). ¹H NMR (300 MHz, DMSO-*d*₆): δ 13.41 (brs, 1 H), 9.25 (brs, 1 H), 8.25 (d, *J* = 8.8 Hz, 1 H), 7.71 (brs, 1 H), 7.41 (dd, *J* = 8.8, 7.3 Hz, 1 H), 7.21–7.15 (m, 2 H), 6.85–6.73 (m, 2 H), 2.41 (s, 3 H). HRMS (ESI) calcd for C₁₆H₁₃N₄O₂S (M + H)⁺, 325.0759; found, 325.0744. Anal. (C₁₆H₁₂N₄O₂S·0.3TFA·0.2CH₃CN) C, H, N.

3-(5-Methylthien-2-yl)-5-(carbamoylamino)indeno[1,2-*c*]pyrazol-4-one (24g). mp >280 °C. ¹H NMR (300 MHz, DMSO-*d*₆): δ 13.65 (brs, 1 H), 9.31 (brs, 1 H), 8.24 (d, *J* = 8.1 Hz, 1 H), 7.79 (brs, 1 H), 7.40 (m, 1 H), 7.05–7.00 (m, 1 H), 7.00–6.92 (m, 1 H), 6.85–6.75 (m, 2 H), 2.53 (s, 3 H). HRMS (ESI) calcd for C₁₆H₁₃N₄O₂S (M + H)⁺, 325.0759; found, 325.0767. Anal. (C₁₆H₁₂N₄O₂S·0.2TFA) C, H, N.

3-(5-Carboethoxythien-2-yl)-5-(carbamoylamino)indeno[1,2-*c*]pyrazol-4-one (24h). mp >280 °C. ¹H NMR (300 MHz, DMSO-*d*₆): δ 9.27 (brs, 1 H), 8.18 (d, *J* = 8.1 Hz, 1 H), 7.85 (brs, 2 H), 7.33 (dd, *J* = 8.1, 7.0 Hz, 1 H), 6.96 (d, *J* = 7.5 Hz, 1 H), 6.75 (brs, 2 H), 4.29 (q, *J* = 7.3 Hz, 2 H), 1.28 (t, *J* = 6.8 Hz, 3 H). HRMS (ESI) calcd for C₁₈H₁₅N₄O₄S (M + H)⁺, 383.0814; found, 383.0788. Anal. (C₁₈H₁₄N₄O₄S·0.5TFA) C, H, N.

3-(Thien-3-yl)-5-(carbamoylamino)indeno[1,2-*c*]pyrazol-4-one (24i). mp >280 °C. ¹H NMR (300 MHz, DMSO-*d*₆): δ 13.65 (brs, 1 H), 9.29 (brs, 1 H), 8.32 (s, 1 H), 8.21 (d, *J* = 8.8 Hz, 1 H), 7.83 (d, *J* = 4.8 Hz, 1 H), 7.77–7.75 (m, 1 H), 7.37 (dd, *J* = 8.1, 7.7 Hz, 1 H), 7.03 (d, *J* = 7.3 Hz, 1 H), 6.76 (brs, 2 H). HRMS (ESI) calcd for C₁₅H₁₁N₄O₂S (M + H)⁺, 311.0603; found, 311.0610. Anal. (C₁₅H₁₀N₄O₂S·0.5TFA·0.01-DMF) C, H, N.

3-(5-Chlorothien-3-yl)-5-(carbamoylamino)indeno[1,2-*c*]pyrazol-4-one (24j). mp >300 °C. ¹H NMR (400 MHz, DMSO-*d*₆, 30 °C): δ 13.70 (brs, 1 H), 9.29 (brs, 1 H), 8.25 (d, *J* = 8.4 Hz, 1 H), 8.19 (d, *J* = 1.5 Hz, 1 H), 7.85 (d, *J* = 1.7 Hz, 1 H), 7.41 (dd, *J* = 8.5, 8.5 Hz, 1 H), 7.07 (d, *J* = 6.8 Hz, 1 H), 6.75 (brs, 2 H). HRMS (ESI) calcd for C₁₅H₁₀N₄O₂SCl (M + H)⁺, 345.0213; found, 345.0209.

3-(2,5-Dimethylthien-3-yl)-5-(carbamoylamino)indeno[1,2-*c*]pyrazol-4-one (24k). mp >280 °C. ¹H NMR (300 MHz, DMSO-*d*₆): δ 13.80 (brs, 1 H), 9.26 (s, 1 H), 8.20 (d, *J* = 8.4 Hz, 1 H), 7.35 (dd, *J* = 8.4, 7.3 Hz, 1 H), 7.11 (brs, 1 H), 7.00 (d, *J* = 7.3 Hz, 1 H), 6.74 (brs, 2 H), 2.52 (s, 3 H), 2.38 (s, 3 H). HRMS (ESI) calcd for C₁₇H₁₅N₄O₂S (M + H)⁺, 339.0916; found, 339.0905. Anal. (C₁₇H₁₅N₄O₂S·0.5TFA) C, H, N.

3-(Furan-2-yl)-5-(carbamoylamino)indeno[1,2-*c*]pyrazol-4-one (24l). mp 278 °C (dec). ¹H NMR (300 MHz, DMSO-*d*₆): δ 13.29 (brs, 1 H), 9.24 (brs, 1 H), 8.21 (d, *J* = 8.8 Hz, 1 H), 7.94 (brs, 1 H), 7.37 (dd, *J* = 8.4, 7.3 Hz, 1 H), 7.21 (d, *J* = 3.3 Hz, 1 H), 7.02 (d, *J* = 6.9 Hz, 1 H), 6.74 (brs, 2 H). HRMS (ESI) calcd for C₁₅H₁₁N₄O₃ (M + H)⁺, 295.0831; found, 295.0838. Anal. (C₁₅H₁₀N₄O₃·1.0TFA) C, H, N.

3-(1-Methylpyrrol-3-yl)-5-(carbamoylamino)indeno[1,2-*c*]pyrazol-4-one (24m). mp >300 °C. ¹H NMR (300 MHz, DMSO-*d*₆): δ 13.20 (brs, 1 H), 9.38 (brs, 1 H), 8.21 (d, *J* = 8.8 Hz, 1 H), 7.61 (dd, *J* = 1.9, 1.8 Hz, 1 H), 7.36 (dd, *J* = 8.8, 8.8 Hz, 1 H), 7.02 (d, *J* = 7.3 Hz, 1 H), 6.88 (dd, *J* = 2.6, 2.2 Hz, 1 H), 6.75 (brs, 2 H), 6.71 (dd, *J* = 6.6, 1.8 Hz, 1 H), 3.71 (s, 3 H). HRMS (ESI) calcd for C₁₆H₁₄N₅O₂ (M + H)⁺, 308.1148; found, 308.1166.

Acknowledgment. We thank Ann Klemm and Marge M. Stafford for their technical expertise. We thank Michael Haas, Wayne Daneker, and Karl Blom for their mass spectroscopic assistance, Gregory Nemeth and Ernest Schubert for their NMR assistance, and Gerry Everlof, Peter Crawford, Mei Li, and Wayne Rankin for their optical spectroscopic assistance. We also thank the staff at DND-CAT, Advanced Photon Source, Argonne National Laboratories for their assistance in X-ray crystallographic data collection.

References

- (1) This work was partially presented at the 218th ACS National Meeting. Seitz, S. P.; Benfield, P. A.; Boylan, J.; Boisclair, M.; Brizuela, L.; Burton, C. R.; Carini, D. J.; Chang, C. H.; Cox, S.; Czerniak, P. M.; Grafstrom, R. H.; Hoess, R. H.; Muckelbauer, J. K.; Nugiel, D. A.; Rossi, K. A.; Trainor, G. L.; Worland, P.; Yue, E. W. *Characterization of Indenopyrazoles as Inhibitors of Cyclin-Dependent Kinases*, 218th ACS National Meeting, New Orleans, LA, Aug 22–26, 1999; American Chemical Society: Washington, DC, 1999; MEDI-316.
- (2) This work was partially presented at the 219th ACS National Meeting. Higley, C. A.; Yue, E. W.; Benfield, P. A.; Burton, K. R. A.; Chang, C.-H.; Cox, S.; Grafstrom, R. H.; Muckelbauer, J. K.; Rossi, K. A.; Seitz, S. P.; Smallwood, A. M.; Chen, H.; Trainor, G. L. *Alkyl-Substituted Indenopyrazoles as Inhibitors of Cyclin-Dependent Kinases*, 219th ACS National Meeting, San Francisco, CA, March 26–30, 2000; American Chemical Society: Washington, DC, 2000; MEDI-039.
- (3) (a) Sielecki, T. M.; Boylan, J. F.; Benfield, P. A.; Trainor, G. L. Cyclin-Dependent Kinase Inhibitors: Useful Targets in Cell Cycle Regulation. *J. Med. Chem.* **2000**, *43*, 1–18. (b) Buolamwini, J. K. Cell Cycle Molecular Targets in Novel Anticancer Drug Discovery. *Curr. Pharm. Des.* **2000**, *6*, 379–392. (c) Meijer, L. Cyclin-Dependent Kinases Inhibitors as Potential Anticancer, Antineurodegenerative, Antiviral and Antiparasitic Agents. *Drug Resist. Updates* **2000**, *3*, 83–88. (d) Sausville, E. A.; Johnson, J.; Alley, M.; Zaharevitz, D.; Senderowicz, A. M. Inhibition of CDKs as a Therapeutic Modality. *Ann. N. Y. Acad. Sci.* **2000**, *910* (Colorectal Cancer), 207–222. (e) Mani, S.; Wang, C.; Wu, K.; Francis, R.; Pestell, R. Cyclin-Dependent Kinase Inhibitors: Novel Anticancer Agents. *Exp. Opin. Invest. Drugs* **2000**, *9*, 1849–1870. (f) Fischer, P. M.; Lane, D. P. Inhibitors of Cyclin-Dependent Kinases as Anti-Cancer Therapeutics. *Curr. Med. Chem.* **2000**, *7*, 1213–1245. (g) Senderowicz, A. M. Small Molecule Modulators of Cyclin-Dependent Kinases for Cancer Therapy. *Oncogene* **2000**, *19*, 6600–6606. (h) Senderowicz, A. M. Development of Cyclin-Dependent Kinase Modulators as Novel Therapeutic Approaches for Hematological Malignancies. *Leukemia* **2001**, *15*, 1–9. (i) Senderowicz, A. M. Cyclin-Dependent Kinase Modulators: A Novel Class of Cell Cycle Regulators for Cancer Therapy. In *Cancer Chemotherapy and Biological Response Modifiers*, Annual 19; Giaccone, G., Schilsky, R., Sondel, P., Eds.; Elsevier Science: New York, 2001; pp 165–188. (j) Roy, K. K.; Sausville, E. A. Early Development of Cyclin Dependent Kinase Modulators. *Curr. Pharm. Des.* **2001**, *7*, 1669–1687. (k) Fischer, P. M. Recent Advances And New Directions In The Discovery And Development Of Cyclin-Dependent Kinase Inhibitors. *Curr. Opin. Drug Discovery Dev.* **2001**, *4*, 623–634.
- (4) Morgan, D. O. Cyclin-Dependent Kinases: Engines, Clocks, and Microprocessors. *Annu. Rev. Cell Dev. Biol.* **1997**, *13*, 261–291.
- (5) Pines, J. Protein Kinases and Cell Cycle Control. *Semin. Cell Biol.* **1994**, *5*, 399–408.
- (6) Hartwell, L. H.; Kastan, M. B. Cell Cycle Control and Cancer. *Science* **1994**, *266*, 1821–1828.
- (7) Kitagawa, M.; Okabe, T.; Ogino, H.; Matsumoto, H.; Suzuki-Takahashi, I.; Kokubo, T.; Higashi, H.; Saitoh, S.; Taya, Y.; Yasuda, H.; Ohba, Y.; Nishimura, S.; Tanaka, N.; Okuyama, A. Butyrolactone I, a Selective Inhibitor of cdk2 and cdc2 Kinase. *Oncogene* **1993**, *8*, 2425–2432.
- (8) Kaur, G.; Stetler-Stevenson, M.; Sebers, S.; Worland, P.; Sedlacek, H.; Myers, C.; Czech, J.; Naik, R.; Sausville, E. Growth Inhibition with Reversible Cell Cycle Arrest of Carcinoma Cells by Flavone L 86-8275. *J. Natl. Cancer Inst.* **1992**, *84*, 1736–1740.
- (9) Czech, J.; Hoffmann, D.; Naik, R.; Sedlacek, H.-H. Antitumoral Activity of Flavone L 86-8275. *Int. J. Oncol.* **1995**, *6*, 31–36.
- (10) Vesely, J.; Havlicek, L.; Strnad, M.; Blow, J. J.; Donella-Deana, A.; Pinna, L.; Letham, D. S.; Kato, J.-Y.; Detivaud, L.; Leclerc, S.; Meijer, L. Inhibition of Cyclin-Dependent Kinases by Purine Analogues. *Eur. J. Biochem.* **1994**, *224*, 771–786.
- (11) Havlicek, L.; Hanus, J.; Vesely, J.; Leclerc, S.; Meijer, L.; Shaw, G.; Strnad, M. Cytokinin-Derived Cyclin-Dependent Kinase Inhibitors: Synthesis and cdc2 Inhibitory Activity of Olomoucine and Related Compounds. *J. Med. Chem.* **1997**, *40*, 408–412.
- (12) De Azevedo, W. F.; Leclerc, S.; Meijer, L.; Havlicek, L.; Strnad, M.; Kim, S.-H. Inhibition of Cyclin-Dependent Kinases by Purine Analogues, Crystal Structure of Human cdk2 Complexed with Roscovitine. *Eur. J. Biochem.* **1997**, *243*, 518–526.
- (13) Meijer, L.; Borgne, A.; Mulner, O.; Chong, J. P. J.; Blow, J. J.; Inagaki, N.; Inagaki, M.; Delcros, J.-G.; Moulinoux, J.-P. Biochemical and Cellular Effects of Roscovitine, a Potent and Selective Inhibitor of the Cyclin-Dependent Kinases cdc2, cdk2, and cdk5. *Eur. J. Biochem.* **1997**, *243*, 527–536.
- (14) Gray, N. S.; Wodicka, L.; Thunnissen, A.-M. W. H.; Norman, T. C.; Kwon, S.; Espinoza, F. H.; Morgan, D. O.; Barnes, G.; LeClerc, S.; Meijer, L.; Kim, S.-H.; Lockhart, D. J.; Schultz, P. G. Exploiting Chemical Libraries, Structure, and Genomics in the Search for Kinase Inhibitors. *Science* **1998**, *281*, 533–538.
- (15) Davis, S. T.; Benson, B. G.; Bramson, H. N.; Chapman, D. E.; Dickerson, S. H.; Dold, K. M.; Eberwein, D. J.; Edelstein, M.; Frye, S. V.; Gampe, R. T., Jr.; Griffin, R. J.; Harris, P. A.; Hassell, A. M.; Holmes, W. D.; Hunter, R. N.; Knick, V. B.; Lackey, K.; Lovejoy, B.; Luzzio, M. J.; Murray, D.; Parker, P.; Rocque, W. J.; Shewchuk, L.; Veal, J. M.; Walker, D. H.; Kuyper, L. F. Prevention of Chemotherapy-Induced Alopecia in Rats by CDK Inhibitors. *Science* **2001**, *291*, 134–137.
- (16) Barvian, M.; Boschelli, D. H.; Cossrow, J.; Dobrusin, E.; Fattaey, A.; Fritsch, A.; Fry, D.; Harvey, P.; Keller, P.; Garrett, M.; La, F.; Leopold, W.; McNamara, D.; Quin, M.; Trumpp-Kallmeyer, S.; Toogood, P.; Wu, Z.; Zhang, E. Pyrido[2,3-d]pyrimidin-7-one Inhibitors of Cyclin-Dependent Kinases. *J. Med. Chem.* **2000**, *43*, 4606–4616.
- (17) Lundgren, K.; Price, S. M.; Excobar, J.; Huber, A. M.; O'Connor, P.; Chong, W.; Duvadie, R.; Li, L.; Chu, S. S.; Nonomiya, J.; Tucker, K.; Mroczkowski, B. Lewis, C. *Novel Cyclin-Dependent Kinase Inhibitors with Potent Growth Inhibitory Action*, 90th AACR National Meeting, Philadelphia, PA, April 10–14, 1999; No. 2022.
- (18) Nugiel, D. A.; Eitzkorn, A.-M.; Vidwans, A.; Benfield, P. A.; Boisclair, M.; Burton, C. R.; Cox, S.; Czerniak, P. M.; Doleniak, D.; Seitz, S. P. Indenopyrazoles as Novel Cyclin Dependent Kinase (CDK) Inhibitors. *J. Med. Chem.* **2001**, *44*, 1334–1336.
- (19) Nugiel, D. A.; Vidwans, A.; Eitzkorn, A.-M.; Rossi, K. A.; Benfield, P. A.; Burton, C. R.; Cox, S.; Doleniak, D.; Seitz, S. P. Synthesis and Evaluation of Indenopyrazoles as Cyclin-Dependent Kinase Inhibitors. 2. Probing the Indeno Ring Substituent Pattern. *J. Med. Chem.* **2002**, *45*, 5224–5232.
- (20) Rotberg, Y. T.; Oshkaya, V. P. Synthesis of 2-Acetyl-1,3-indanediones Substituted in the Benzene Ring. *J. Org. Chem. USSR (Engl. Transl.)* **1972**, *8*, 86–88.
- (21) Meijer, L.; Thunnissen, A.-M. W. H.; White, A. W.; Garnier, M.; Nikolic, M.; Tsai, L. H.; Walter, J.; Cleverley, K. E.; Salinas, P. C.; Wu, Y. Z.; Biernat, J.; Mandelkow, E.-M.; Kim, S.-H.; Pettit, G. R. Inhibition of Cyclin-Dependent Kinases, GSK-3 β and CK1 by Hymenialdisine, a Marine Sponge Constituent. *Chem. Biol.* **2000**, *7*, 51–63.
- (22) Dreyer, M. K.; Borcherding, D. R.; Dumont, J. A.; Peet, N. P.; Tsay, J. T.; Wright, P. S.; Bitonti, A. J.; Shen, J.; Kim, S.-H. Crystal Structure of Human Cyclin-Dependent Kinase 2 in Complex with the Adenine-Derived Inhibitor H717. *J. Med. Chem.* **2001**, *44*, 524–530.
- (23) Shewchuk, L.; Hassell, A.; Wisely, B.; Rocque, W.; Holmes, W.; Veal, J.; Kuyper, L. F. Binding Mode of the 4-Anilinoquinazoline Class of Protein Kinase Inhibitor: X-ray Crystallographic Studies of 4-Anilinoquinazolines Bound to Cyclin-Dependent Kinase 2 and p38 Kinase. *J. Med. Chem.* **2000**, *43*, 133–138.
- (24) Legraverend, M.; Tunnah, P.; Noble, M.; Ducrot, P.; Ludwig, O.; Grierson, D. S.; Leost, M.; Meijer, L.; Endicott, J. Cyclin-Dependent Kinase Inhibition by New C-2 Alkynylated Purine Derivatives and Molecular Structure of a CDK2–Inhibitor Complex. *J. Med. Chem.* **2000**, *43*, 1282–1292.
- (25) Schulze-Gahmen, U.; Brandsen, J.; Jones, H. D.; Morgan, D. O.; Meijer, L.; Vesely, J.; Kim, S.-H. Multiple Modes of Ligand Recognition: Crystal Structures of Cyclin-Dependent Protein Kinase 2 in Complex with ATP and Two Inhibitors, Olomoucine and Isopentenyladenine. *Proteins: Struct., Funct., Genet.* **1995**, *22*, 378–391.
- (26) Hoessel, R.; Leclerc, S.; Endicott, J. A.; Nobel, M. E. M.; Lawrie, A.; Tunnah, P.; Leost, M.; Damiens, E.; Marie, D.; Marko, D.; Niederberger, E.; Tang, W.; Eisenbrand, G.; Meijer, L. Indirubin, the Active Constituent of a Chinese Antileukaemia Medicine, Inhibits Cyclin-Dependent Kinases. *Nat. Cell Biol.* **1999**, *1*, 60–67.
- (27) DeBondt, H. L.; Rosenblatt, J.; Jancarik, J.; Jones, H. D.; Morgan, D. O.; Kim, S.-H. Crystal Structure of Cyclin-Dependent Kinase 2. *Nature* **1993**, *363*, 595–602.
- (28) Schulze-Gahmen, U.; De Bondt, H. L.; Kim, S.-H. High-Resolution Crystal Structures of Human Cyclin-Dependent Kinase 2 with and without ATP: Bound Waters and Natural Ligand as Guides for Inhibitor Design. *J. Med. Chem.* **1996**, *39*, 4540–4546.
- (29) Wick, S. T.; Dubay, M. M.; Imanil, I.; Brizuela, L. Biochemical and Mutagenic Analysis of the Melanoma Tumor Suppressor Gene Product/p16. *Oncogene* **1995**, *11*, 2013–2019.
- (30) Carlson, B. A.; Dubay, M. M.; Sausville, E. A.; Brizuela, L.; Worland, P. J. Flavopiridol Induces G1 Arrest with Inhibition of Cyclin-Dependent Kinase (CDK) 2 and CDK4 in Human Breast Carcinoma Cells. *Cancer Res.* **1996**, *56*, 2973–2978.
- (31) Xu, X.; Nakano, T.; Wick, S.; Dubay, M.; Brizuela, L. Mechanism of Cdk2/Cyclin E Inhibition by p27 and p27 Phosphorylation. *Biochemistry* **1999**, *38*, 8713–8722.

- (32) Rosenblatt, J.; DeBondt, H.; Jancarik, J.; Morgan, D. O.; Kim, S.-H. Purification and Crystallization of Human Cyclin-Dependent Kinase 2. *J. Mol. Biol.* **1993**, *230*, 1317–1319.
- (33) Otwinowski, Z.; Minor, W. Processing of X-ray Diffraction Data Collected in Oscillation Mode. In *Methods in Enzymology, Macromolecular Crystallography, Part A*; Carter, C. W., Jr., Sweet, R. M., Eds.; Academic Press: New York, 1997; Vol. 276, pp 307–326.
- (34) Kissinger, C. R.; Gehlhaar, D. K.; Fogel, D. B. Rapid Automated Molecular Replacement by Evolutionary Search. *Acta Crystallogr.* **1999**, *D55*, 484–491.
- (35) Brunger, A. T.; Adams, P. D.; Clore, G. M.; Delano, W. L.; Gros, P.; Grosse-Kunstleve, R. W.; Jiang, J.-S.; Kuszewski, J.; Nilges, M.; Pannu, N. S.; Read, R. J.; Rice, L. M.; Simonson, T.; Warren, G. L. Crystallography and NMR System: A New Software Suite for Macromolecular Structure Determination. *Acta Crystallogr.* **1998**, *D54*, 905–921.
- (36) Skehan, P.; Storeng, R.; Scudiero, D.; Monks, A.; McMahon, J.; Vistica, D.; Warren, J. T.; Bokesch, H.; Kenney, S.; Boyd, M. R. New Colorimetric Cytotoxicity Assay for Anticancer-Drug Screening. *J. Natl. Cancer Inst.* **1990**, *82*, 1107–1112.

JM0201722